

**STUDY OF DYNAMIC EFFECTS IN MICROPARTICLE
ADHESION USING ATOMIC FORCE MICROSCOPY**

A Thesis

by

ANSHUL KAUSHIK

Submitted to the Office of Graduate Studies of
Texas A&M University
in partial fulfillment of the requirements for the degree of

MASTER OF SCIENCE

December 2004

Major Subject: Mechanical Engineering

**STUDY OF DYNAMIC EFFECTS IN MICROPARTICLE
ADHESION USING ATOMIC FORCE MICROSCOPY**

A Thesis

by

ANSHUL KAUSHIK

Submitted to Texas A&M University
in partial fulfillment of the requirements
for the degree of

MASTER OF SCIENCE

Approved as to style and content by:

Arun Srinivasa
(Chair of Committee)

K. R. Rajagopal
(Member)

J. Walton
(Member)

Dennis O'Neal
(Head of Department)

December 2004

Major Subject: Mechanical Engineering

ABSTRACT

Study of Dynamic Effects in Microparticle Adhesion Using Atomic Force
Microscopy. (December 2004)

Anshul Kaushik, B.E., Osmania University, Hyderabad, India

Chair of Advisory Committee: Dr. Arun Srinivasa

The adhesion and removal of particles from surfaces is a contemporary problem in many industrial applications like Semiconductor manufacturing, Bioaerosol removal, Pharmaceuticals, Adhesives and Petroleum industry. The complexity of the problem is due to the variety of factors like roughness, temperature, humidity, fluid medium etc. that affect pull-off of particles from surfaces. In particle removal from surfaces using fluid motion, the dynamic effects of particle separation will play an important role. Thus it is essential to study the dynamic effects of particle removal. Velocity of pull-off and force duration effects are two important dynamic factors that might affect pull-off. Particle adhesion studies can be made using the Atomic Force Microscope (AFM). The velocity of pull-off and force duration can be varied while making the AFM measurements. The objective of the current work is to obtain the dependence of pull-off force on pull-off velocity. Experiments were conducted using AFM and the data obtained from the experiments is processed to obtain plots for pull-off force vs. particle size and pull-off force vs. pull-off velocity. The pull-off force is compared with the

predictions of previous contact adhesion theories. A velocity effect on pull-off force is observed from the experiments conducted.

To

My parents and loving sister

ACKNOWLEDGEMENTS

I would like to take this opportunity to offer my heartfelt thanks to a number of people without whose help and support this thesis would never have been possible. I must start with my advisor Dr. Arun Srinivasa, for providing me with an opportunity to work with him. He has always guided me through my work and at the same time given me enough freedom to learn and produce original ideas. I would also like to express my gratitude to Dr. Denis Phares for his invaluable ideas.

I would like to thank Dr. William Lackowski and Yulia Vasilyeva for providing me with training and support for doing the experiments on the Atomic Force Microscope at their Material Characterization Facility.

My parents have provided me with countless opportunities for which I am extremely grateful. The love that my sister and I share in my life is invaluable to me. Nothing I say here can do justice to the continuous and unending support I get from my family. I must also thank a few friends who have been with me through the ups and downs in my life. Thank you very much Praveena, Shruti, Purna and Raghu.

Last but not the least it gives me immense pleasure to thank the numerous friends who have come into my life at various stages to make it wonderful. Thank you Jaya, Srilatha, Srinivas, Sudharshan, John, Srikanth, Raghavendra, Mini, Anu, Vidhya and Prathyusha. I shall always remember the good times I had with you all.

TABLE OF CONTENTS

	Page
ABSTRACT.....	iii
DEDICATION.....	v
ACKNOWLEDGEMENTS.....	vi
LIST OF FIGURES	ix
CHAPTER I. INTRODUCTION	1
1.1 Micro-particle pull-off: Introduction and applications	1
1.2 Various factors affecting pull-off	4
1.3 Importance of pull-off velocity and force duration on pull-off	7
1.4 Theory	8
1.5 Introduction to force measurement methods	8
CHAPTER II. OVERALL SCOPE AND OBJECTIVES	14
2.1 Overall scope	14
2.2 Objectives	15
CHAPTER III. MEASURING MICROPARTICLE PULL-OFF USING ATOMIC FORCE MICROSCOPY	16
3.1 Description of the Atomic Force Microscope (AFM)	16
3.2 Materials and apparatus	20
3.3 Adhesion of particles to cantilevers.....	21
3.4 Experimental procedure.....	30
CHAPTER IV. PREVIOUS THEORIES AND MODELS	33
4.1 Introduction to various theories	33
4.2 JKR theory	34
4.3 DMT theory	37
4.4 Calculation of interaction due to Van der Waals forces	38
4.5 Model for deformable bodies.....	41
4.6 Calculation of stiffness for spherical particle	44
4.7 Stiffness and mass for a given set of particle and cantilever	47

CHAPTER V. RESULTS AND DISCUSSION.....	49
5.1 Pull-off forces for particles of various sizes at a single frequency	49
5.2 Pull-off force for varying frequency	51
5.3 Discussion.....	53
REFERENCES	55
VITA.....	59

LIST OF FIGURES

	Page
FIG. 1. Effect of friction on contact area.....	5
FIG. 2. Schematic diagram of the JKR Apparatus.	10
FIG. 3. Schematic diagram of the Surface Force Apparatus.	12
FIG. 4. Measurement of the deflection of the cantilever tip.....	17
FIG. 5. Measurement of lateral forces using Atomic Force Microscope.	18
FIG. 6. Motion of the tip over the surface in force mode.	19
FIG. 7. Figures showing the protocol of gluing the particles to the cantilever. ...	25
FIG. 8. Figures showing different views of the cantilever with particle on it.	28
FIG. 9. A figure of the scale used to measure the size of the particles.....	29
FIG. 10. Software interface for Force mode.....	30
FIG. 11. A sample force-displacement curve obtained from the software.	32
FIG. 12. Contact between two spheres of radii R_1 and R_2 under a normal load P_0 .	35
FIG. 13. Stress distribution in the contacting spheres.	35
FIG. 14. Interaction of a single molecule with an infinite surface.	39
FIG. 15. Interaction of a sphere with an infinite surface.	40
FIG. 16. Model for rigid particle.	42
FIG. 17. Free body diagrams of (a) particle, (b) cantilever and (c) surface.	43
FIG. 18. Figure to show the (a) undeformed and (b) deformed particle.....	44
FIG. 19. Plot of pull-off force vs. particle size.	50
FIG. 20. Cantilever with particle. The cantilever had excess glue on the bottom face.....	50

FIG. 21.	Pull-off force Vs. Frequency for a particle of diameter 17.156 μm	51
FIG. 22.	Pull-off Force Vs. Frequency for particles of varying sizes.....	52
FIG. 23.	Plot of the constant 'Pull-off force/ Particle size' Vs. Frequency.....	53

CHAPTER I

INTRODUCTION

1.1 Micro-particle pull-off: Introduction and applications

The interaction of micro particles with a surface is of interest to a diverse range of topics relating to powder transport, air pollution and surface contamination. Many industrial processes rely on either the efficiency to remove particles from surfaces or a technique to hold particles in place on a surface. Some examples of such processes are listed here:

1. *Semiconductor manufacturing*: In Semiconductor industry, one of the primary causes of failure during fabrication is the contamination of semiconductor surfaces by colloidal particles. At present 30-40% of the microprocessor chips manufactured turn out to be defective due to surface contamination (1). Several methods such as solvent baths, sprays, megasonic and brush cleaning are in extensive use for cleaning of these semiconductor surfaces. For the proper functioning of these methods, a thorough understanding of forces of interaction and the underlying mechanism of particle detachment at the fundamental level is required.

This thesis follows the style and format of the *Journal of Colloid and Interface Science*.

2. *Bioaerosol detection and removal:* Most medical procedures and equipment require extremely clean environments, which are rid of any bacteria or viruses. These bacteria and viruses need to be removed from all surfaces and from air. Detection and removal of these bacteria from air is critical for complete cleaning of the whole environment. Also for cleaning of the surface a complete understanding of adhesion of these bacteria to any surface in use is necessary.
3. *Trace explosives detection:* Explosives when being developed require a fine powder of the chemical explosive, in order to burn easily. These powders usually adhere to outside surfaces of the explosive container and other surrounding surfaces. In explosives detection, all surfaces are tested for traces of these explosive powders by chemical means. For the test, the surfaces are wiped for any powders using a paper and then this paper is checked for traces of the explosive. In order to understand this process fully, a thorough understanding of the particle adhesion to various surfaces is necessary.
4. *Pressure Sensitive Adhesives:* Pressure sensitive adhesives can be defined as a category of adhesive tapes that in dry form are aggressive and permanently tacky at room temperatures. These will adhere to a surface when applied with pressure and do not require activation by water heat or solvents. These properties are obtained by mixing high molecular weight elastomers with small bulky molecules called tackifiers. Therefore, to study the mechanism

of tackification an understanding of its interaction with any surface is required. Such studies were previously done using AFM (2).

5. *Pharmaceuticals*: Drugs are most commonly developed and stored as powders. These powders need to be stored under controlled conditions so that they do not react with the surrounding medium. Also these particles should be readily released when consumed. A great level of understanding of particle interaction between drug particles and various plastic and biological surfaces at various conditions like temperature, humidity and chemical conditions is necessary for drugs to function normally. Particle studies for pharmaceutical applications were made previously (3, 4).
6. *Membrane filtration*: The use of membranes to separate solutes from liquids is a recent development in process engineering and environmental protection. These advanced filtration processes use polymeric or organic films as membranes. In these processes, the deposition of solutes or dispersed materials on the membrane surface, membrane fouling, plays an important role in determining the overall process performance (5). Such deposits are often colloidal in nature and thus the study of adhesive properties of these materials is necessary.
7. *Xerography*: The usual process of making copies involves a multistage process. The toner is first transferred from a toner reservoir to a rotating photoconductive layer, where it should adhere to places depending on the copy to be made. Subsequently the particles are transferred to a rotating

rubber transport belt and finally onto clean paper, where it is fused by applying pressure and elevated temperatures. Therefore in order to achieve an optimal copy, the adhesion of toner particles to various surfaces must be carefully tuned (6). Thus the study of toner particle interactions with various surfaces involved, at the working temperature ranges is necessary for the process to work successfully. (include figure if necessary)

8. *Petroleum industry:* In petroleum industry, the problem of particles getting trapped in fluid flow is encountered. During the production of crude oil, colloidal particles become entrained in the flowing fluid near the wellbore and plug constricted pore channels of the oil bearing rock formations. This can dramatically reduce the permeability of the flowing hydrocarbons (1). Many surfactants are often used to prevent colloidal particles from becoming entrained. For the formation of these surfactants, the study of particle detachment mechanism in these fluids becomes extremely important.

1.2 Various factors affecting pull-off

There are many factors that affect the pull-off of particles from surfaces. These factors pertain to the particle, the surface, the fluid medium and the environment. Each of these factors might be more important than any other in different cases. Many studies have been made studying the importance of these factors.

1. *Surface roughness:* At the submicron scale, surface topography becomes extremely important. Machined surfaces are not flat, and surface roughness is known to decrease particle adhesion by reducing the contact area (7). This is seen in Fig. 1 below. Many measurements of particle adhesion over rough surfaces have been made (8 - 12). In a comparison of AFM tip pull-off over peaks and valleys in a rough surface (5), it was found that the pull-off force was much smaller at the peak than the valley.

The surface roughness of the particle also might play an important role in the adhesion. Material inhomogeneities also play an important part in particle adhesion (12).

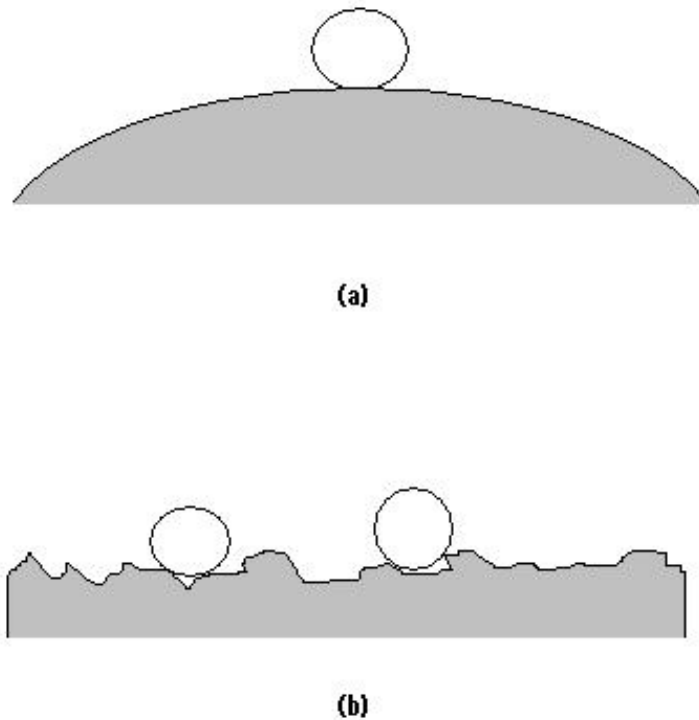


FIG. 1. Effect of friction on contact area. (a) smooth surface and (b) rough surface.

2. *Material of the particle and the surface:* The adhesion is directly dependent on various material properties. The molecular density of the material directly determines the Van der Waals force of adhesion (13). The surface energy dictates the force of adhesion between the particle and the surface. The elastic modulus of the materials dictates how much the particle and the surface will deform under the action of adhesive forces (14).
3. *The fluid medium:* Many practical applications require the study of particle adhesion in different fluid media, because many times the adhesion occurs inside a fluid medium, rather than in air. The properties of the fluid surrounding the particle and the surface affect the pull-off. The properties like fluid surface energy, ionic strength, the PH value (1, 10) and surface tension (4) of the fluid play a part in the adhesion.
4. *Humidity:* The effect of humidity on adhesion is necessary for applications which are not always confined to closed and controlled environments. Humidity affects on particle adhesion have been studied (15). This study was made using the surface force apparatus on mica over rough gold films. It revealed that the pull-off force increased with relative humidity.
5. *Temperature:* The effect of temperature is of particular importance to pharmaceutical applications. The adhesion of particles is strongly influenced by the viscoelastic property of the particle material (16) and the elasticity of a material is affected by temperature. Temperature effects have been studied in previous work (3). In this work, the adhesion properties of

polyethyleneglycol 4000 and heavy precipitated calcium carbonate particles to a characterized stainless steel surface at various temperatures. It was observed that the median adhesion force increased with increase in temperature.

6. *Size of the particle:* The particle size directly influences the force of adhesion due to Van der Waals energies (13). The contact area between the particle and the surface, which directly influences the adhesion force due to surface energy (17, 18), is also dependent on the particle size. Effect of particle size is studied in (19).

1.3 Importance of pull-off velocity and force duration on pull-off

Suspension or resuspension of particles exposed to a moving fluid is a common occurrence in nature. In many applications the removal of particles from a surface occurs by perturbations due to fluid flow. Therefore the particle detachment mechanism will not necessarily be by the application of a static pull-off force, perpendicular to the surface. These forces may be at an angle to the surface. In addition these forces might be changing in intensity and direction with time.

The dynamic effects of particle detachments need to be studied in order to completely understand the resuspension of particles in moving fluid. Critical components of study of dynamic effects are pull-off velocity and duration of application of the pull-off force. In order to completely understand the dynamic effects, these aspects of particle suspension need to be studied.

1.4 Theory

Physical interactions between macroscopic bodies or molecules are primarily described by interaction energies. They can also be described in terms of forces, which can be measured directly as described in the next section. The forces between particles and surfaces can be calculated on the basis of pair wise additive intermolecular forces. By adding up these pair wise interaction forces of interacting macroscopic bodies for various geometries, such as flat parallel surfaces, spheres, cylinders or combination of these geometries (13), the net interaction energies and the corresponding forces can be expressed in a closed form, using geometrical parameters such as radius and separation distance. However the form of intermolecular potential and the number density of the interacting molecules must be known for the materials.

There are various theories that predict the pull-off of particles. Some of these theories are discussed in chapter 4 of this thesis.

1.5 Introduction to force measurement methods

The adhesion forces between surfaces and particles can be measured directly by various methods like Sensitive force transducers in contact mechanics (JKR apparatus), Surface force apparatus and Atomic force Microscope etc. Some of them are described below.

JKR apparatus for force measurements in contact mechanics (20): This apparatus is used to measure the adhesion force between a particle and a surface in contact. The apparatus is illustrated in Fig 2.

Essentially it consists of a lower sample holder, which is placed on a balance to measure the load (force) on the sample. The upper sample holder is connected to a precision translation stage. This stage interfaces with the host computer to get commands and send displacement information measured by a displacement sensor. This apparatus can be sealed in a thermal and humidity control chamber. The contact diameter between the samples is measured by a camera placed on top of the upper sample.

To conduct the experiments, the upper sample is brought close to the lower sample at controlled speed. When the distance becomes comparable to the range of intermolecular forces, the surfaces jump into contact. At this point the displacement counter can be set to zero. This position shows a negative reading on the balance. Now the sample can be moved down to any specified distance and radius of contact and load readings can be taken at each displacement.

Then the sample is again moved up and radius of contact and load at each value of displacement are measured. The snap off will occur at a negative displacement. The load value at snap off can be noted as the adhesion force.

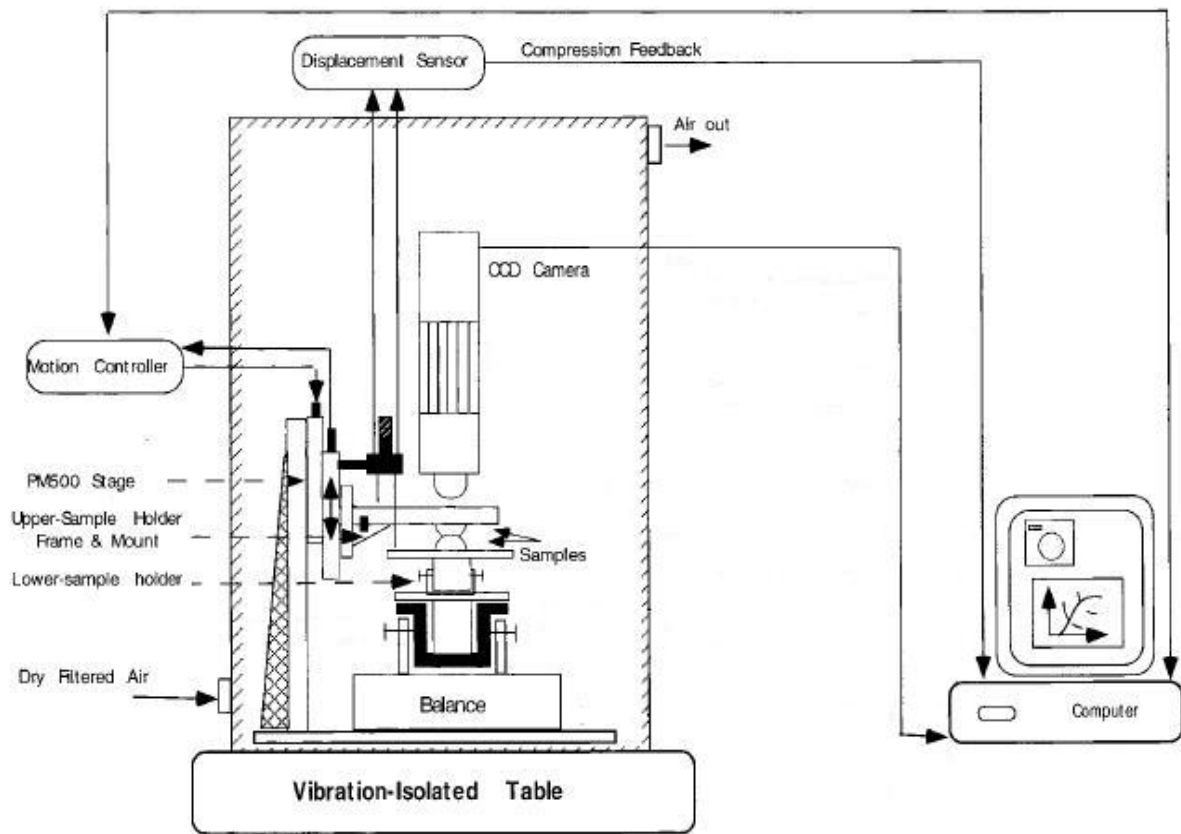


FIG. 2. Schematic diagram of the JKR Apparatus.

The process of bringing the sample up can be done at various speeds to study the dynamic effects of unloading. This apparatus can also be used to measure the surface energy of the surfaces by maintaining the contact in equilibrium state during loading process. The drawback of this method being that it cannot be used for micron size particles. The optical resolutions and load measuring mechanism are suitable only for macroscopic bodies.

Surface force apparatus (13): In the surface force apparatus, the force between two surfaces in controlled vapors or immersed in liquids can be directly measured. A schematic of the apparatus is shown in Fig. 3. The distance resolution is about 0.1 nm and the force sensitivity is about 10^{-8} N.

The SFA essentially consists of two curved molecularly smooth surfaces of mica of radius $R \approx 1$ cm, between which the interaction forces are measured using a variety of interchangeable force measuring springs. The separation between the two surfaces is measured by optical means, based on interference fringes. The distance between the two surfaces is controlled by the use of a three stage mechanism of increasing sensitivity. The coarse control (upper rod) allows positioning to within 1 μm , the medium control (lower rod) allows positioning to about 1 nm and finally the piezoelectric crystal tube is used for positioning to 0.1 nm.

Now force between the surfaces can be measured by expanding or contracting the piezoelectric crystal by a known amount and then measuring optically how much the surfaces actually moved. The difference when multiplied with the stiffness of the force measuring spring gives the force.

Modified versions have been developed, which have extended the SFA method to opaque materials, replacing the optical technique for measuring distance by a capacitance method, the overall accuracy remaining the same. Again this apparatus is not suitable for micron size particles.

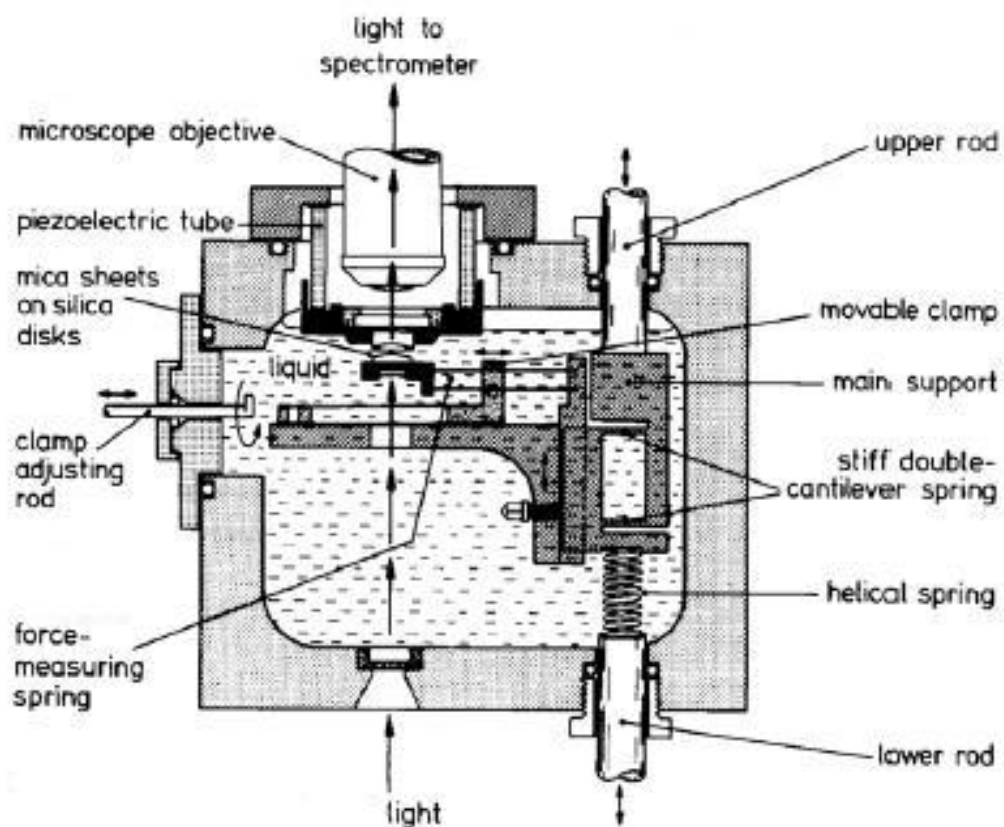


FIG. 3. Schematic diagram of the Surface Force Apparatus.

Atomic Force Microscope (AFM): AFM was invented in 1980s (21) as a technique for imaging surface topography from micrometer to nanometer length scales. At the same time, the apparatus allows one to measure forces, precisely and accurately, in various liquid and gaseous media and at controlled temperatures. Thus AFM is an excellent method to characterize surface topography of various surfaces and to quantitatively study the micro-particle adhesion forces for these

surfaces. The current work applies the principles of the AFM to particle adhesion studies.

The principle of working of the Atomic Force Microscope is measuring the forces between a sharp pyramidal tip and the sample surface. The tip is attached to a cantilever spring. This tip is usually raster scanned over the surface to record the surface topography. The topography can be imaged with a sub-nanometer resolution. To do adhesion measurements, the tip is moved over the surface perpendicular to it. The deflection (force) of the cantilever can be recorded as a function of the cantilever displacement over the surface. This plot is known as force-displacement curve. Detailed working and apparatus has been described in section 3.1.

Now if a particle is attached to the bottom face of the cantilever spring, in place of the tip and the experiment is conducted in a similar fashion as described above, the force of adhesion of the particle to the surface can be measured. This procedure was used to conduct the experiments in this work.

CHAPTER II

OVERALL SCOPE AND OBJECTIVES

2.1 Overall Scope

In the study of microparticle adhesion to surfaces, various factors explained in section 1.2 are of importance. Using the AFM, many of these factors can be studied. The tests can be done for various surfaces of different roughness and compositions. AFM allows tests to be conducted in various media like open air, gases and fluids. For testing with fluid medium, a special apparatus called the fluid cell is used. Additionally, the humidity and temperature of the surface and the environment can be controlled by external means.

The process of attaching the particles to cantilevers enables us to study the pull-off forces required for these particles on various surfaces in controlled conditions. Particles of different materials and sizes can be tested on. The roughness of the particles will vary with the composition of the particle material.

Lateral forces i.e. forces required to move the tip parallel to the surface can be measured using the AFM. These studies can be carried out by measuring the torsional deflection of the cantilever tip.

2.2 Objectives

The work in this thesis concentrates on the effects of pull-off velocity and force duration on pull-off force. This work is necessary to study the dynamic effects of particle pull-off. In this work, Polystyrene particles of sizes ranging from 6 microns to 25 microns have been attached to cantilever tips and tests have been conducted on stainless steel surfaces.

To test the effect of pull-off velocity, these tests were done at varying frequencies, ranging from 1 Hz to 30 Hz. This frequency is limited by the working frequency of the equipment.

The results of these tests will be compared with the models available in previous literature and conclusions will be made.

CHAPTER III

MEASURING MICROPARTICLE PULL-OFF USING ATOMIC FORCE MICROSCOPY

3.1 Description of the Atomic Force Microscope (AFM)

Since its invention in 1986 (21), the AFM has been a useful tool for imaging surface topography and adhesion force measurements in various gaseous and liquid media and at controlled temperatures. It was invented as an application of the Scanning Tunneling Microscope (STM) (22).

STM relies on tunneling current between the probe and the sample to sense the topography of the sample. A sharp metal tip (in best case, atomically sharp), is positioned a few atomic diameters above a conducting sample, which is electrically biased with respect to the tip. At a distance of under 1 nanometer, a tunneling current will flow from the sample to the tip. This tunneling current varies exponentially with the tip-sample separation. Thus by sensing the tunneling current, the sample separation can be estimated from the exponential relation between the current and the separation. The use of this method is however limited to conducting materials.

The AFM works by monitoring the elastic deformation of a cantilever spring as it is moved over the surface, following various profiles. This deformation of the cantilever is monitored by measuring the movement of a laser which is directed to

a sensor, after reflecting from the top surface of the cantilever, as shown in Fig. 4.

This sensor gives the output in volts.

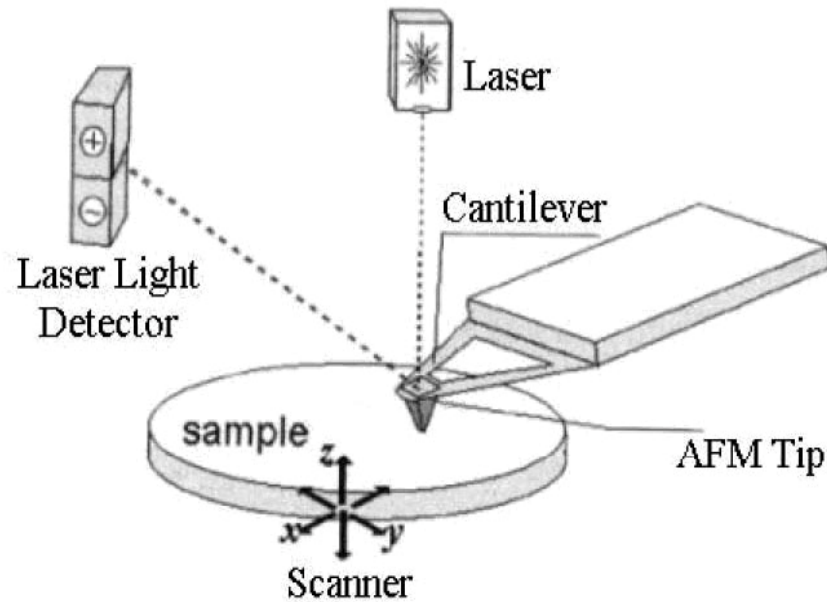


FIG. 4. Measurement of the deflection of the cantilever tip.

AFM for imaging surface topography: The most widely used application of the AFM is to image the surface topography. For this, the cantilever with the tip is raster scanned over the surface, parallel to the surface. As it moves over the surface, the deformations on the surface cause the tip to deflect up or down depending on whether the formation is a peak or valley. These deflections of the cantilever are noted at each point over the surface and thus by techniques of raster scan, the whole surface can be imaged.

AFM for measuring lateral forces: To measure the lateral forces to move the tip over the surface, the torsional stiffness of the cantilever tip needs to be known.

The tip can be moved over the surface, parallel to the surface and as it moves, the movement of the laser beam in the horizontal direction can be noted. This horizontal movement of the laser can be related to the deflection angle of the tip. This deflection angle is a measure of the lateral force required to move the tip. This is seen in Fig. 5.

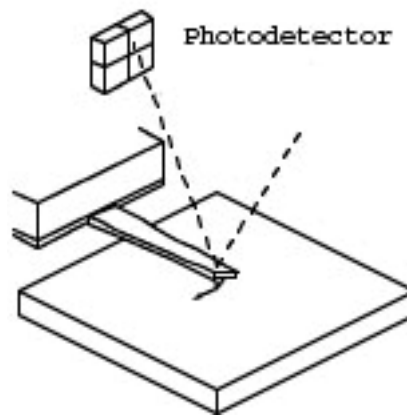


FIG. 5. Measurement of lateral forces using Atomic Force Microscope.

AFM for measuring pull-off forces: Measurement of pull-off forces using AFM can be achieved by moving the cantilever up and down, perpendicular to the surface being tested. The deflections of the tip are noted at each position of the tip over the surface, by measuring the movement of the laser on the sensor. The process of the cantilever approaching the surface is called extending and that of moving away from the surface is called retracting. This sequence is shown in detail in Fig. 6 and described below.

1. *Extending:* The tip first approaches the substrate with no cantilever deflection ('**ab**' of the Fig. 6). At some critical separation distance, the

cantilever “snaps to contact” and is deflected downwards (**bc** in the Fig. 6). As the cantilever continues to approach the substrate, it is pressed down against the substrate and deflects upwards (**cd** in the Fig. 6).

2. *Retracting:* When the tip is pulled away from the surface, the upward deflection of the cantilever is reduced (**de** in the Fig. 6). Beyond the equilibrium point (labeled **e**), the cantilever continues to be deflected downwards as an upward force is applied. This is seen in **ef** in Fig. 6. At point **f**, the deflection of the cantilever causes enough upward force to pull-off the tip from the surface. Therefore at this point, the tip snaps off from the surface as seen in **fg** in figure 2. Thereafter, the cantilever moves over the tip without any deflection, seen in **gh**.

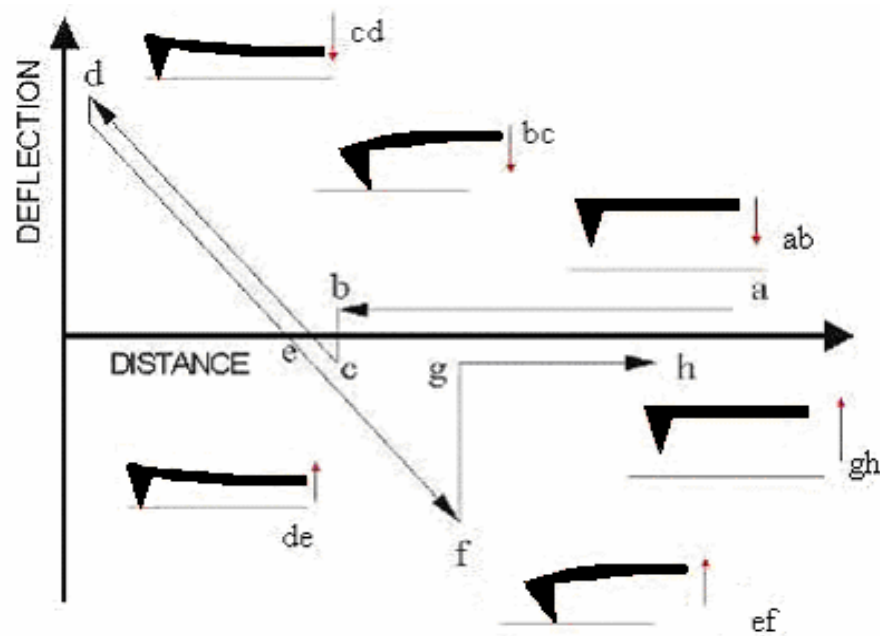


FIG. 6. Motion of the tip over the surface in force mode.

This sequence of extending and retracting is repeated over the surface at desired frequency to get a plot of deflection of the tip vs. the displacement of the tip seen in the Fig. 6 above. The deflection ' \mathbf{fg} ', corresponding to the snap off when multiplied with the stiffness of the cantilever, gives the required pull-off force.

3.2 Materials and apparatus

Particles: The particles used in this study were Polystyrene spheres. These particles were obtained from Duke Scientific. The size range of the particles is 1 to 50 microns.

Substrate: The surface used to conduct the experiment was a 430 stainless steel surface (Ted Pella Inc.).

Atomic Force Microscope: The AFM used here is a Digital Instruments Nanoscope IIIa Scanning Probe Microscope, equipped with a 'J' scanner. The instrument produces x and y motion by movement of the tip over the surface, using a manual manipulator and z motion by movement of the substrate, using a piezo electric controller. It is equipped with digital camera, which gives continuous streaming video output to an independent monitor. The images from this camera have a total maximum magnification of 1000X. This camera is also capable of taking still images.

Cantilever Tips: The cantilever tips used in the experiments were obtained from Veeco Systems. These are Silicon Nitride tips. The cantilevers have gold coating on top for better reflection. These cantilevers come in four sizes, lengths

100 and 200 micron, widths 40 micron (wide) and 15 micron (narrow). The spring constants of the cantilevers are specified by the manufacturer and are given in Table 1.

TABLE 1
Cantilever stiffness values

Cantilever type	Stiffness (N/m)
100 microns wide legs	.58
100 microns narrow legs	.38
200 microns wide legs	.12
200 microns narrow legs	.06

Adhesive: The selection of the adhesive used to glue the particles to the cantilever tips is critical. The glue used for this operation in our work is LOCTITE QuickTite^R from Manco Inc..

3.3 Adhesion of particles to cantilevers

The process of making the force-distance measurements on particles using AFM was first done by Ducker et al. in 1991 (23). They had made these measurements for silica particles. Subsequent work with an AFM using microparticles has been used to study numerous processes and applications (4, 5, 8, 9, 10, 12, 24 -31). The selection of adhesives and the process used are described in these works. The choice of the adhesive depends, among other things, on the nature

of the particle material, the experimental medium (liquid or air), the cantilever material, the temperature at which the experiment is conducted and on the method of fastening.

Detailed fastening procedure is described by Claesson et al. (32). Essentially a micromanipulator or an XYZ-translation stage is used to attach particles to a cantilever. First, a small amount of heat-sensitive adhesive is warmed up. The end of a small wire is brought into contact with the adhesive by means of the XYZ-translation stage. The amount of glue is then reduced by repeatedly touching it with the dry parts of the glass slide. Then it is transferred to the end of a cantilever which is heated on a hot plate. Finally a second wire covered with particles is brought into contact with the cantilever. Rolling of the particle in the adhesive should be prevented in this step and the cantilever should be removed from the hotplate immediately. These operations take place under an optical microscope.

In our work, a different protocol was designed for attaching particles to cantilever tips. The key steps involved in this protocol are:

1. Putting a controlled amount of glue in the vicinity of the particle and
2. Moving the tip rapidly to over the glue and then over to the particle, before the glue dries.

To accomplish the first task, a right combination of the glue and a glue carrying medium is required. Carbon fibers of submicron diameters were chosen to carry the glue to the required place near the chosen particle. These fibers were wound together to make a strand of about 15 microns diameter. This was found

useful because this strand absorbed any excess glue and only dispersed small amounts of glue when touched over the surface.

The glue chosen was QuickTite^R from LOCTITE. This glue was chosen because it was of desired viscosity and the setting time was around 20 seconds which was enough for completion of all the steps involved.

To move the cantilever rapidly between the glue and the particle, essentially a micromanipulator or a XYZ-translation stage is required. For this purpose, the mounting stage provided with the AFM was found satisfactory as the cantilever could be rigidly mounted on it and moved over the stage in X, Y and Z directions. To glue the particles, the following protocol is observed

1. A big selection of the particles is spread on a glass slide. A jet of dry Nitrogen is blown over the slide so that any lumps of particles are removed and the particles get dry. This slide is now kept under the microscope. (Fig. 7a)
2. By moving the slide around, a particle of required size is selected.
3. Now the cantilever is mounted in its seat and by the use of the translation stage, it is brought near the selected particle. (Fig 7b)
4. A small amount of glue is put upon the carbon fibers. The carbon fibers absorb any excess glue and only a small amount of glue is present on the surface. Carbon fibers used here are seen in Fig. 7c.
5. This glue tipped carbon fiber strand is brought in the vicinity of the selected particle and the tip. This fiber is touched to the glass slide and a small

amount of glue is deposited near the particle (Fig. 7d). It is critical that the glue does not engulf the particle and the tip. To ensure this, the selection of the carbon fibers was made.

6. Now the cantilever is moved rapidly over to the glue on the glass slide and brought down so that a small amount of glue is deposited on the bottom side of the cantilever. Again it needs to be ensured that the cantilever does not get into too much contact with the glue and get excess glue, which will engulf the particle, or get glue on the top surface, which will hamper the reflection of laser from the top surface of the cantilever. Also if it gets too much glue onto it, the stiffness of the cantilever might change by a huge margin which is unacceptable.
7. Now this cantilever with the glue on its bottom face is moved over to the selected particle and brought into contact with the top of the particle (Fig. 7e). It is now allowed to stay in this position for some time so that the glue hardens and a bond is formed. The cantilever, with the particle, is now lifted up from the glass slide.
8. A jet of dry nitrogen is blown over the cantilever and if the particle stays on the cantilever, it is assumed that the bonding is good.
9. The cantilever with the particle is now stored in a closed container for around 24 hours so that the glue solidifies completely.

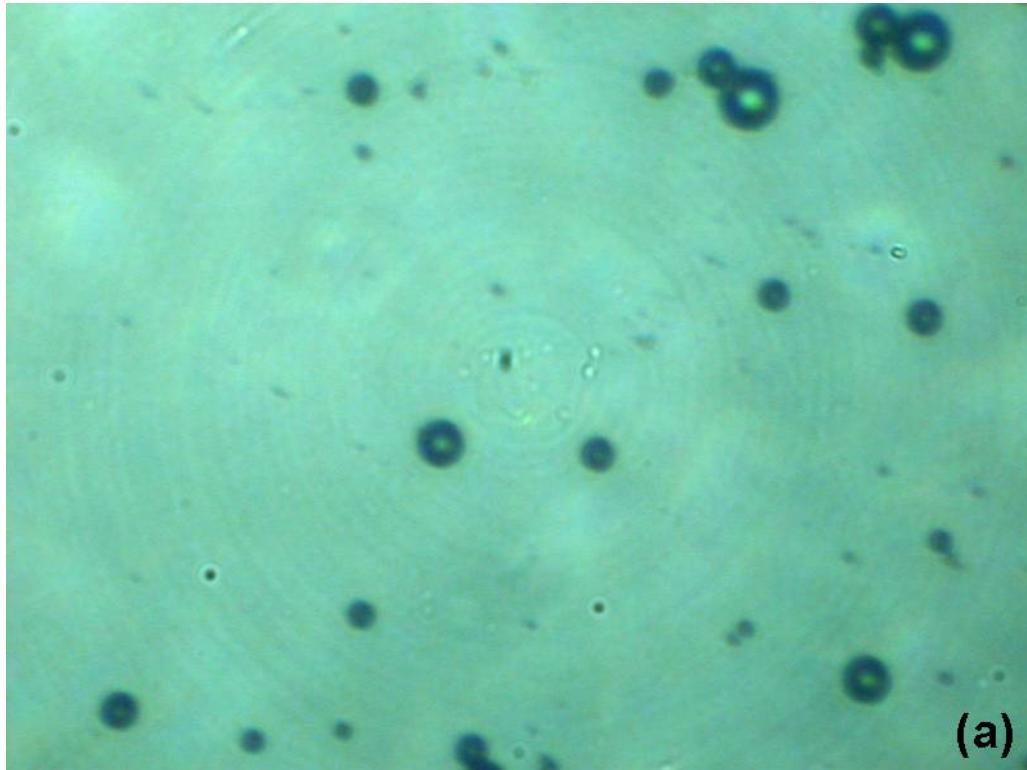


FIG. 7. Figures showing the protocol of gluing the particles to the cantilever. (a) Particles spread out on a glass plate, (b) The cantilever brought near the selected particle using the precision translation stage, (c) The strand made using carbon fibers of sub-micron diameter, (d) A blob of glue deposited near the particle and (e) The cantilever lowered onto the particle after getting the glue on its lower surface.

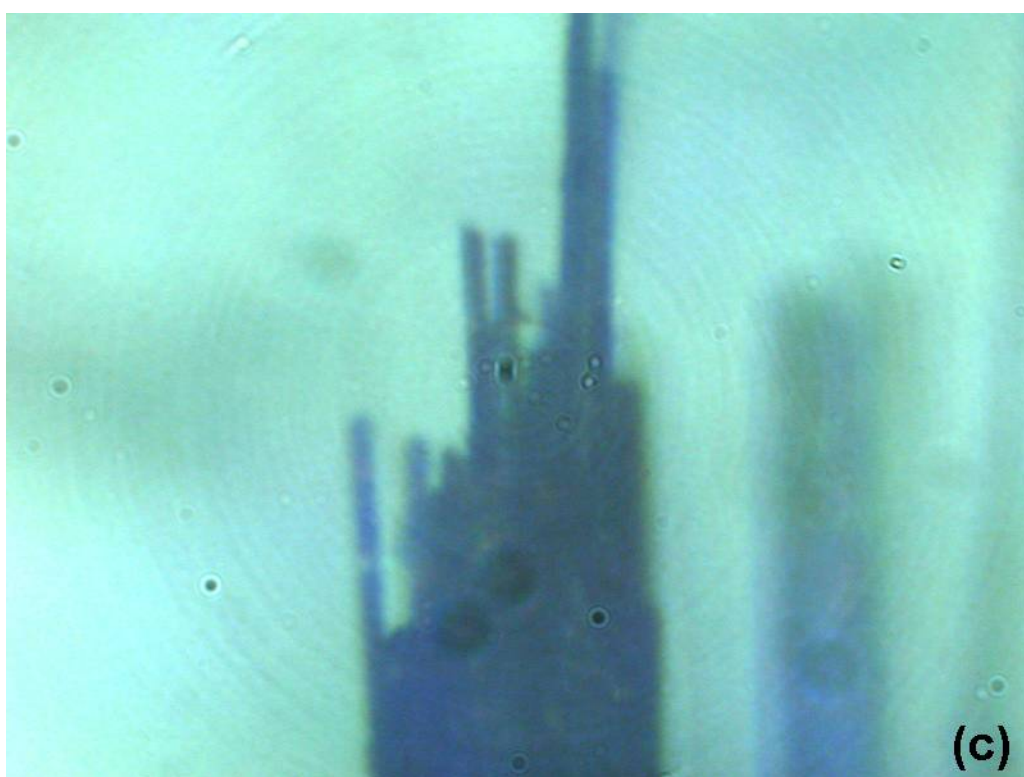
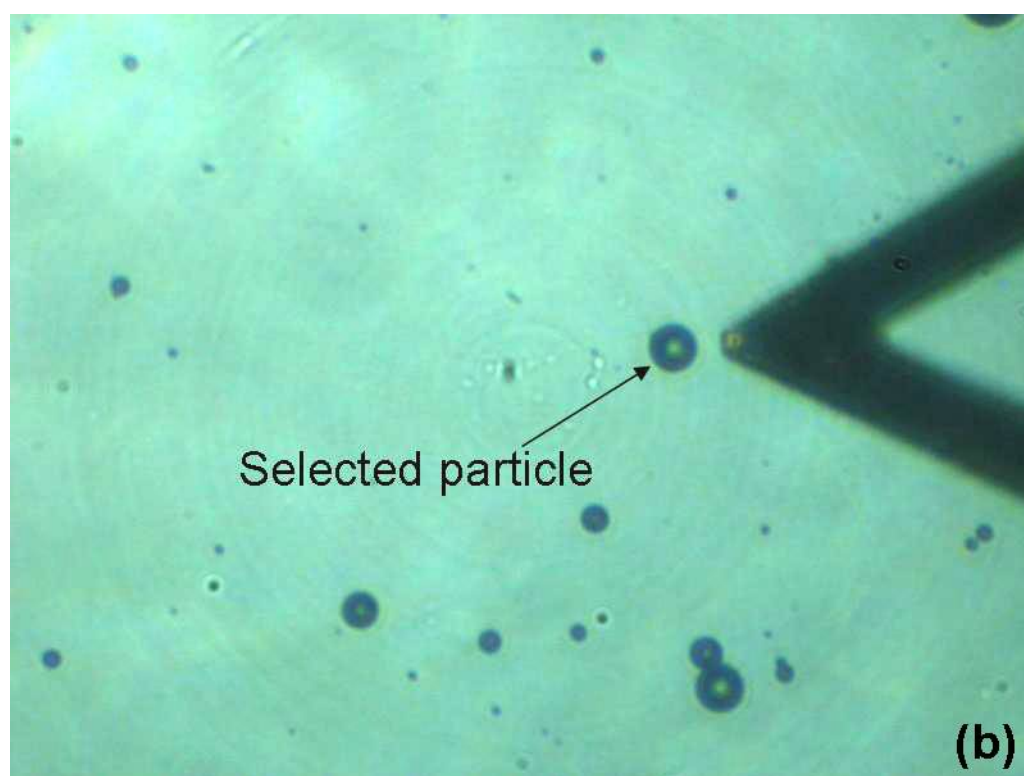


FIG. 7. Continued

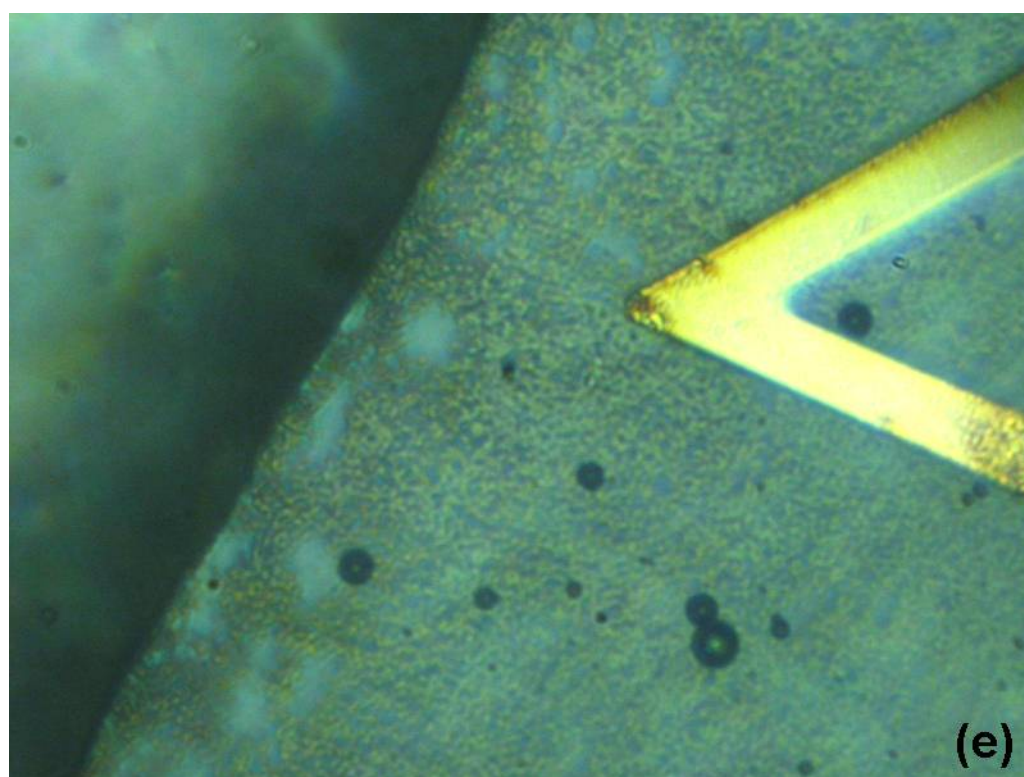
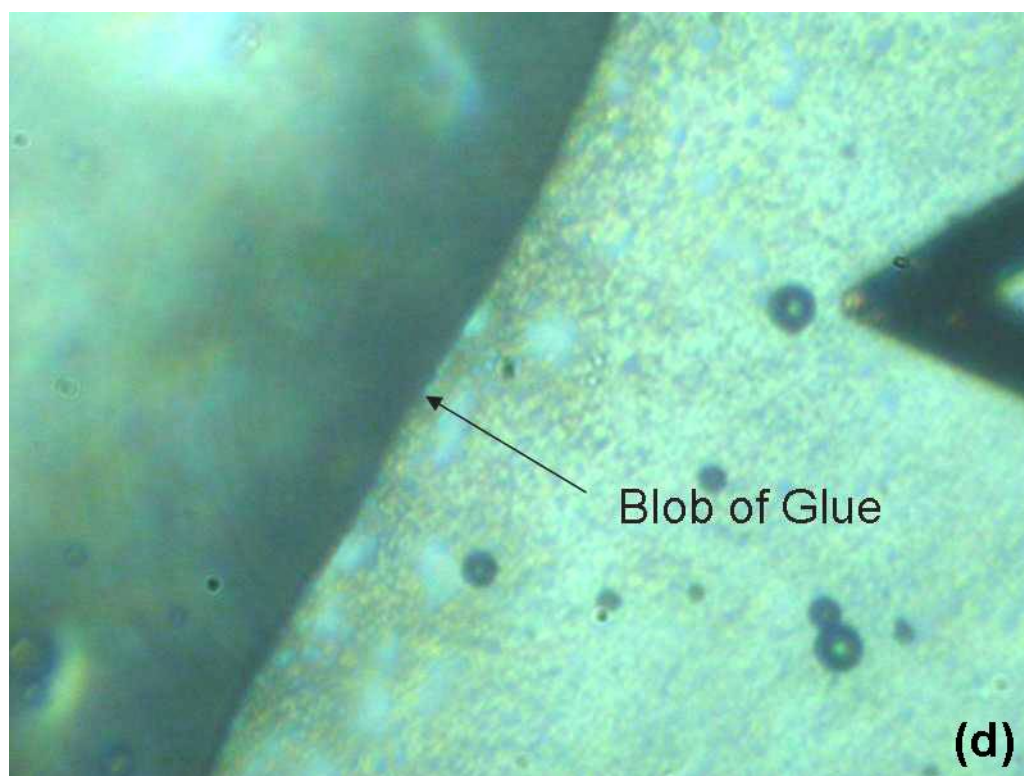


FIG. 7. Continued

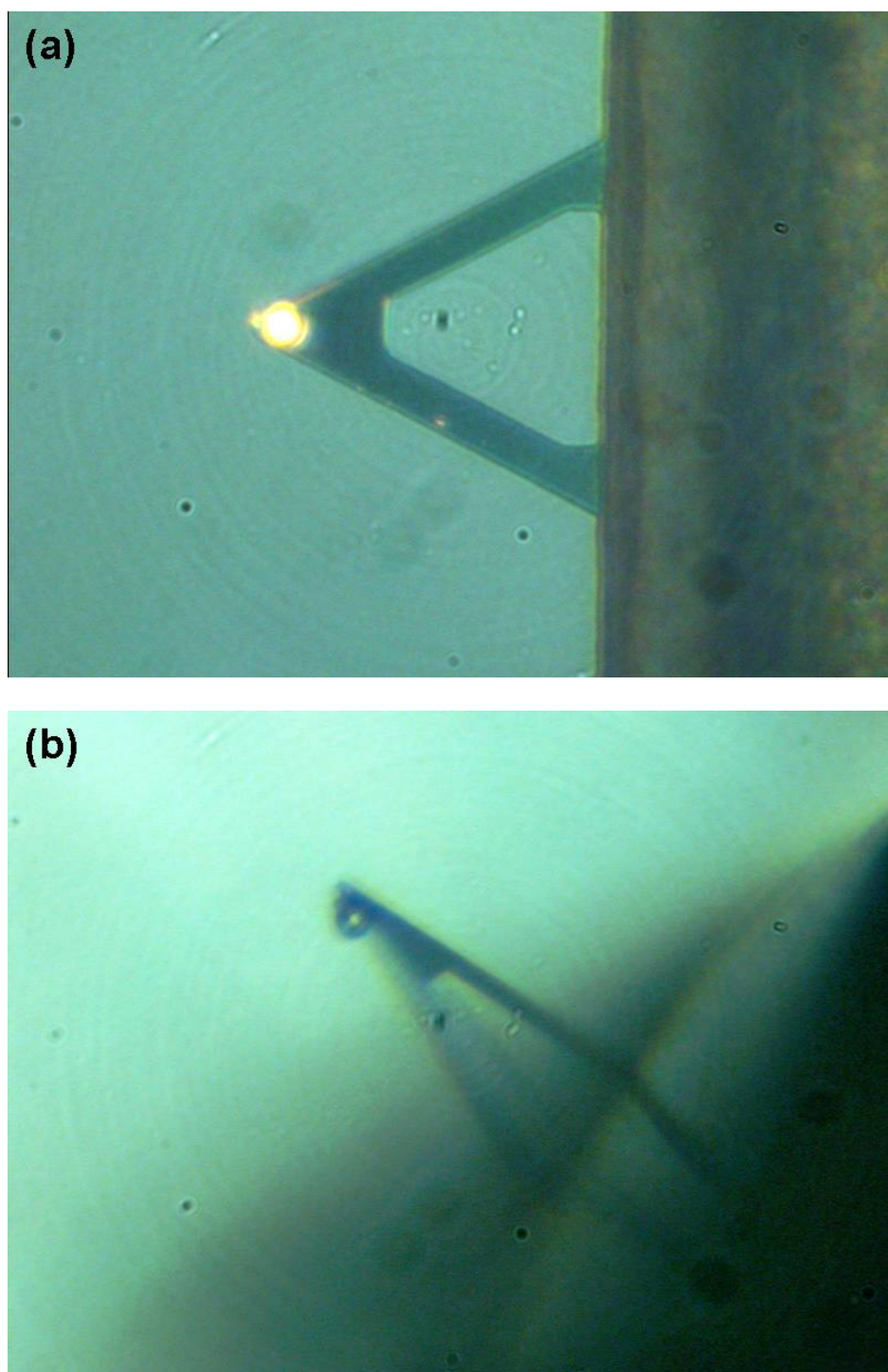


FIG. 8. Figures showing different views of the cantilever with particle on it. (a) Cantilever is horizontal and (b) Cantilever is held at an angle to the vertical axis to show the depth of the particle

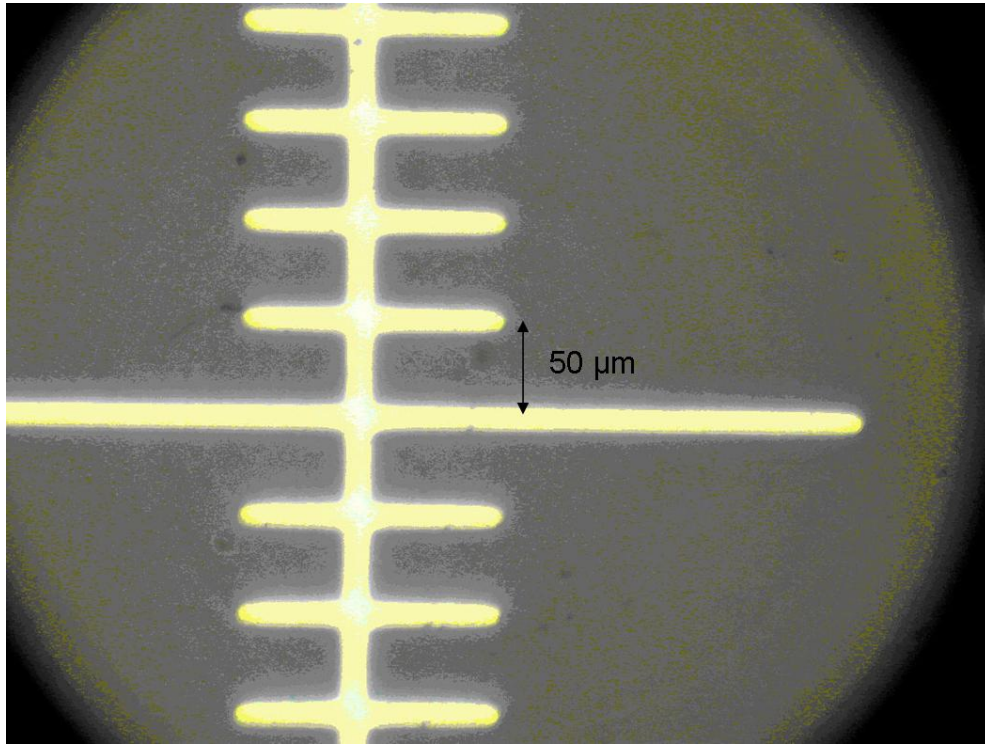


FIG. 9. A figure of the scale used to measure the size of the particles. The smallest unit on the scale is 50 μm .

This tip with particle is now ready to do experiments upon. Some views of the cantilever with the particle are seen in Figs. 8a and 8b. The size of the particle can be measured by using a scale, whose smallest unit is 50 μm . To measure the size, an image of the particle is taken using the camera provided with the microscope and at the same magnification, an image of the scale is also taken. Now by measuring the length of the both the particle and the smallest unit on the scale, and then taking their ratio, the size of the particle can be determined. An image of the scale used here is seen in Fig. 9.

3.4 Experimental procedure

The main interface between the user and the AFM is through the software provided with the AFM. This software allows the user to use the instrument in many modes. The mode required for the required measurements is contact mode. The software interface for contact mode can be seen in Fig. 10 below.

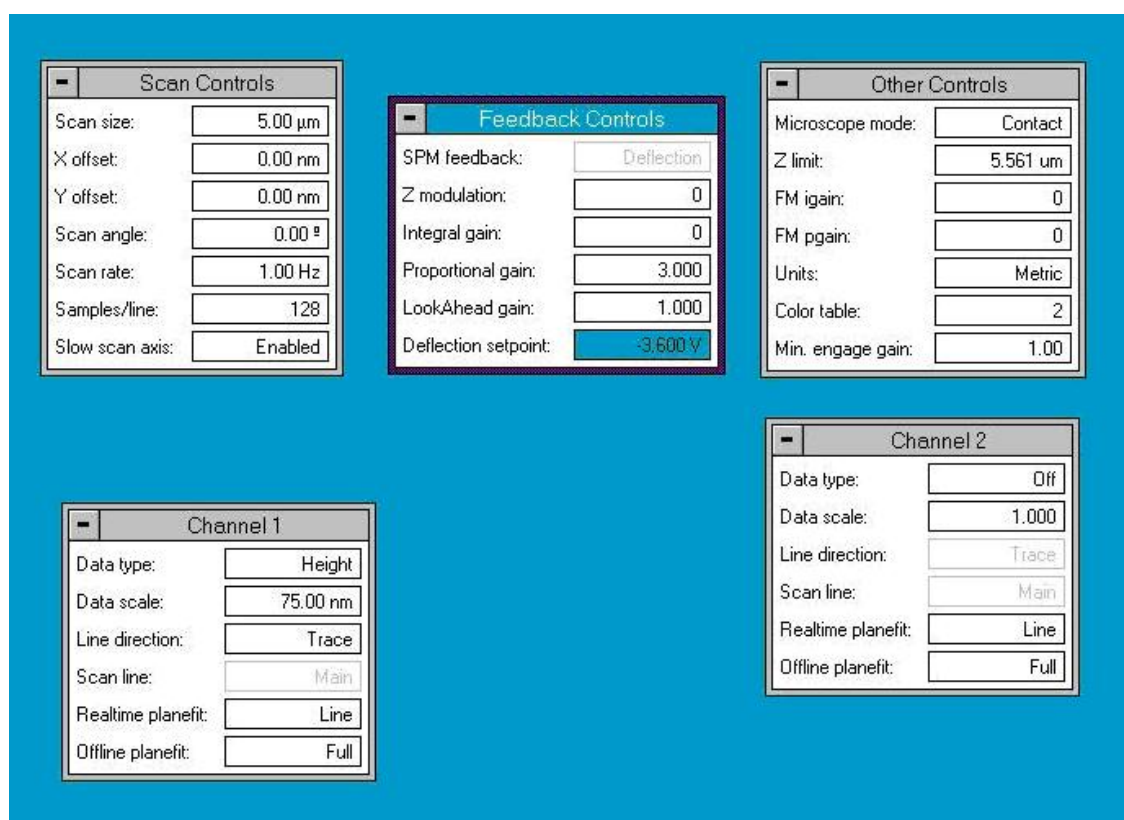


FIG. 10. Software interface for Force mode.

The surface to be tested is first cleaned with acetone so that it is rid of all dirt, oils and coatings. It is now dried with a jet of dry Nitrogen and placed on the XYZ-translation stage of the AFM. The cantilever with the particle on its tip is mounted in the tip holder and placed over the surface to be tested so that the bottom of the particle is about 1 mm above the surface. The laser is now directed to the tip of the cantilever. This is reflected to the light detection sensor. The sensor is moved up or down to get the reflection to the center of the sensor. This is seen as 0 Volts reading from the sensor.

The engage command is given to the software now. This starts to move the tip down steadily till the reading from the sensor reaches a pre-determined set-point voltage, which tells the software that engagement with the surface has occurred. This voltage is generally set to 2 V above the value which the sensor showed when the tip was stationary. This value of 2 V was determined by trial and error. For softer materials, the set-point needs to be higher to detect engagement with the surface.

When the software shows that engagement with the surface is done, it needs to be given a 'force mode' command. This command turns it to the mode which gives the force-displacement curves as output. Now the output from the software shows the force-displacement curves for the given particle. One sample output can be seen in Fig. 11. These curves can be stored to the system disk using the capture command.



FIG. 11. A sample force-displacement curve obtained from the software.

The main aim of the experiments is to measure the pull-off force at various pull-off velocities. The pull-off velocity of the particle is directly proportional to the frequency at which the extending and retracting cycle is repeated. In the software, there is a provision to change this frequency.

Now for each particle, the experiment is conducted at varying frequencies and the force-displacement plot is saved for each frequency. From these plots, the force is calculated for each frequency, by multiplying the maximum deflection with the spring constant. These forces can now be plotted with respect to frequency.

CHAPTER IV

PREVIOUS THEORIES AND MODELS

4.1 Introduction to various theories

Various theories predict adhesion force of particles over surfaces. There are mainly two types of forces. Contact forces and short range (molecular) forces. Contact has been studied in detail in previous works (17, 18, 33 - 36). The Hertz theory calculated the shape and size of the zone of contact due to the elastic deformation of two bodies in contact. The JKR and DMT theories start with the Hertz contact and consider the effects of adhesion force on the deformation of the sphere to determine the contact area and pull-off force.

Molecular forces arise due to various properties of molecules (13). Coulomb forces act between charged particles. Electrostatic interactions due to dipole moments act on polarized molecules in presence of electric fields emanating from nearby molecules. In addition to these forces, some forces act between all molecules, even totally neutral ones. These are most commonly referred to as dispersion forces. These contribute the most to Van der Waals forces as they are always present, irrespective of the type of molecule.

4.2 JKR theory

This work was published in 1971. It attempts to include the effect of adhesion force on the deformation of two elastic spheres in contact. According to Hertz theory, two spheres of radii R_1 and R_2 pressed together under a load P_0 will have a contact radius a_0 , shown in Fig. 12, given by

$$a_0^3 = \frac{3}{4} \pi (k_1 + k_2) \frac{R_1 R_2}{R_1 + R_2} P_0, \text{ where } k_i = \frac{1 - \nu_i^2}{\pi E_i}$$

Two distant points in the spheres approach each other by an amount δ given by

$$\delta^3 = \frac{9}{16} \pi^2 (k_1 + k_2) \frac{R_1 + R_2}{R_1 R_2} P_0^2$$

But the equations of Hertz contact are not valid when adhesive forces act between the two bodies. It is assumed that the contact radius will increase to a_1 as shown in Fig. 12, because of the adhesive forces. The total load increases to P_1 , because of an additional load due to adhesion (called the Hertz load). It assumes a stress distribution as shown in curve B in Fig. 13. This distribution assumes compressive stress in the center and tensile stress near the contact boundary. The curves A and C are Hertz stress for contact radii a_1 and a_0 respectively.

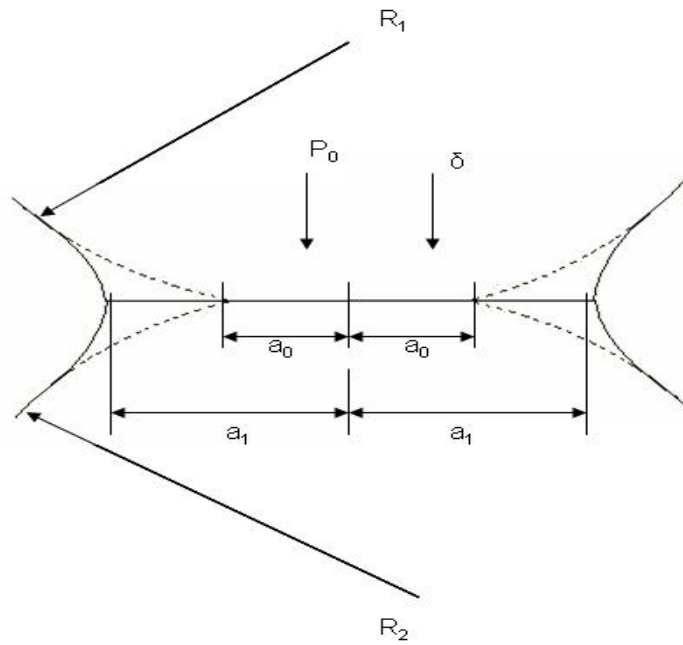


FIG. 12. Contact between two spheres of radii R_1 and R_2 under a normal load P_0 . The dotted line is contact assumed by Hertz and solid line is contact given by JKR theory.

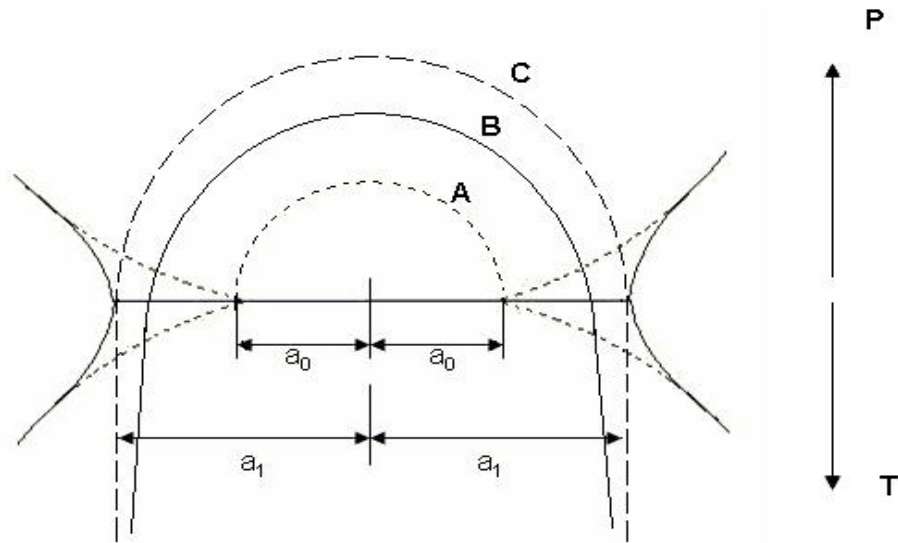


FIG. 13. Stress distribution in the contacting spheres. Distribution A is Hertz stress with contact radius a_0 , B is the actual distribution assumed in JKR theory and C is Hertz stress with contact radius a_1 .

Essentially, equilibrium between these two spheres will be attained when the differential of the total energy in the system U_T with respect to the contact radius a will reach zero. Total energy is the sum of three terms, the stored elastic energy, the mechanical energy in the applied load and the surface energy. On calculation, for two spheres of same material, this total energy U_T is found to be

$$U_T = \frac{1}{K^{\frac{2}{3}} R^{\frac{1}{3}}} \left[\frac{1}{15} P_1^{\frac{5}{3}} + \frac{1}{3} P_0^2 P_1^{-\frac{1}{3}} \right] - \frac{1}{K^{\frac{2}{3}} R^{\frac{1}{3}}} \left[\frac{1}{3} P_0 P_1^{\frac{2}{3}} + \frac{2}{3} P_0^2 P_1^{-\frac{1}{3}} \right] - \gamma \pi (R P_1 / K)^{\frac{2}{3}}$$

where,

$$R = R_1 R_2 / (R_1 + R_2)$$

γ is the surface energy of both the spheres

$$K = \frac{4}{3\pi(k_1 + k_2)} \cdot P_1 \text{ and } P_0 \text{ are as defined before.}$$

Now for equilibrium, $dU_T / da_1 = 0$, which is equivalent to $dU_T / dp_1 = 0$.

This on simplification gives

$$P_1 = P_0 + 3\gamma\pi R + \sqrt{(P_0 + 3\gamma\pi R)^2 - P_0^2}$$

Therefore the contact radius a which is defined as $a^3 = \frac{RP}{K}$, is given by

$$a^3 = \frac{R}{K} [P + 3\gamma\pi R + \sqrt{6\gamma\pi RP + (3\gamma\pi R)^2}]$$

Now as the load P is reduced, a decreases. For real solution to be obtained for this equation, P has to be greater than $-\frac{3}{2}\gamma\pi R$. This implies that separation will occur at

$$P = -\frac{3}{2}\gamma\pi R$$

This is the pull-off force required to separate a particle of radius R given by JKR theory. The negative sign just signifies that the force is in upward direction.

4.3 DMT theory

The DMT theory takes into account the interaction forces outside the contact area. But these interaction forces are assumed not to deform the profile, which remains Hertzian. It is assumed that pull-off occurs at zero contact radius. The important results of this theory are given here.

The contact radius of the sphere with the surface under zero load is given by

$$a_0^3 = \frac{2\pi\gamma R^2}{K} \text{ where } \gamma \text{ is the surface energy of both the surfaces, } R \text{ is the radius of}$$

the sphere and K is defined as

The pull-off force, reached at zero contact radius is given by $F_{pull-off} = 2\pi\gamma R$ where, γ is the surface energy of the particle and the surface and R is the radius of the sphere.

4.4 Calculation of interaction due to Van der Waals forces

In this section, the total interaction force between a particle and a surface is found using the principle of addition of the interaction forces.

According to the theory developed on the basis of dipole-induced dipole interactions for neutral molecules, the energy of interaction between two molecules is given by [ref]

$$W(r) = -\frac{3\alpha_0^2 h\nu}{4(4\pi \epsilon_0)^2 r^6}, \text{ where}$$

α_0 is the polarizability of the Bohr atoms,

h is the Planks constant,

ν is the orbiting frequency of the electron,

ϵ_0 is the permittivity of free space and

r is the distance between the two molecules.

To find the interaction between a particle and a surface, we first integrate this energy of interaction over the surface to get the interaction between a molecule and the surface and then integrate over all the molecules in the particle to get the total interaction. For convenience, it is assumed that $W(r) = -C / r^n$.

Consider the surface to be composed of circular rings of cross sectional area $dx \cdot dz$ and radius x as shown in Fig. 14. The total volume of the ring is $2\pi x dx dz$, and the number of molecules in the ring will be $2\pi \rho x dx dz$ where ρ is the number density of the molecules in the surface.

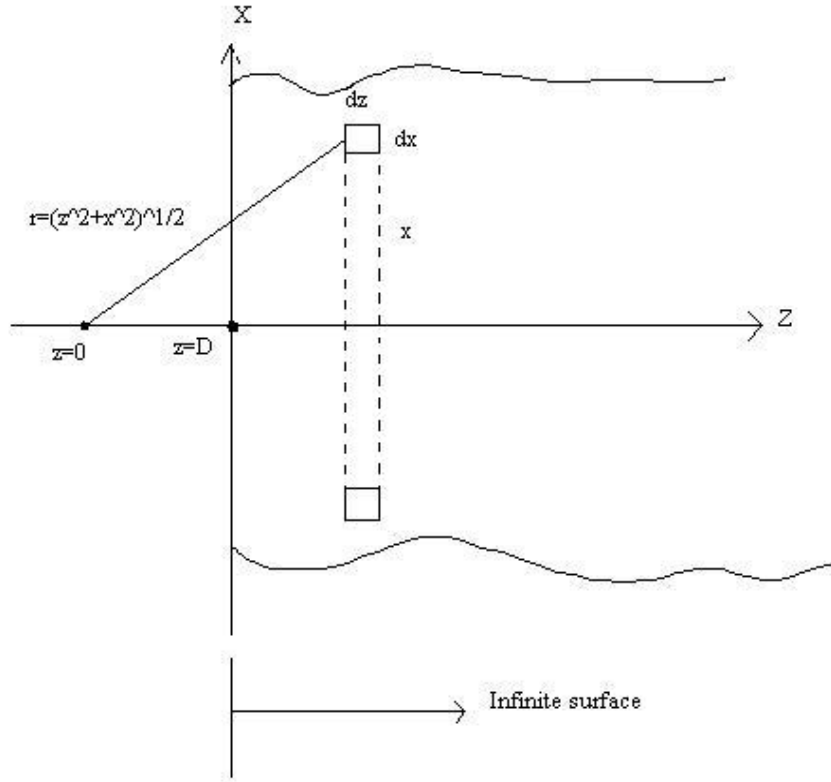


FIG. 14. Interaction of a single molecule with an infinite surface. The surface is assumed to be composed of rings of radius 'x' at a distance of 'z' from the molecule.

The net interaction energy of a single molecule at a distance D from the surface will be given by,

$$W(D) = -2\pi C\rho \int_{z=D}^{z=\infty} dz \int_{x=0}^{x=\infty} \frac{xdx}{(z^2 + x^2)^{n/2}}$$

$$= \frac{2\pi C\rho}{(n-2)} \int_D^{\infty} \frac{dz}{z^{n-2}} = -2\pi C\rho / (n-2)(n-3) D^{n-3}$$

Using this interaction between a molecule and a surface, we go do the calculation for a large sphere of radius R and the surface. Consider the sphere to be

composed of solid rings of thickness dz at a distance $D+z$ and of radius x , as shown in Fig. 15.

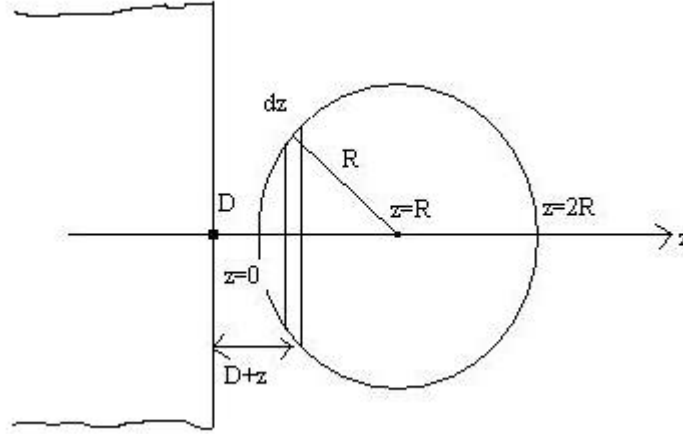


FIG. 15. Interaction of a sphere with an infinite surface. The sphere is assumed to be composed of solid disks of thickness dz at a distance $D+z$ from the surface.

From the chord theorem, we have $x^2 = (2R - z)z$. The volume of the thin disc is $\pi x^2 dz = \pi(zR - z)z dz$. Therefore the number of molecules in the disc is $\pi \rho(zR - z)z dz$, where ρ is the density of molecules in the sphere material. As all these molecules are at a distance $(D + z)$, we have the interaction energy as,

$$W(D) = -\frac{2\pi^2 C \rho^2}{(n-2)(n-3)} \int_{z=0}^{z=2R} \frac{(2R-z)z dz}{(D+z)^{n-3}}$$

For $D \ll R$, only small values of z contribute to the integral. Therefore,

$$W(D) = -\frac{2\pi^2 C \rho^2}{(n-2)(n-3)} \int_0^\infty \frac{2Rz dz}{(D+z)^{n-3}}$$

$$= -\frac{4\pi^2 C \rho^2 R}{(n-2)(n-3)(n-4)(n-5)D^{n-5}}$$

For $n=6$, as we had started, $W(D) = -\pi^2 C \rho^2 R / 6D$. This is the interaction potential between a sphere of radius R and a surface. The force of interaction is given by $F = \partial W(D) / \partial D$. Therefore

$$F = \pi^2 C \rho^2 R / 6D^2, \text{ where}$$

$$C = \frac{3\alpha_0^2 h\nu}{4(4\pi \epsilon_0)^2}$$

ρ is the molecule number density of the sphere and surface materials.

R is the radius of the sphere

D is the distance between the surface and the point in the sphere, nearest to the surface.

Therefore, the force of interaction between a sphere and a surface is given by $F = \pi^2 C \rho^2 R / 6D^2$.

4.5 Model for deformable bodies

The model currently being developed is a lumped mass model as shown in Fig. 16. The cantilever is replaced by a spring of spring constant K_3 and an equivalent mass M_3 . The particle is approximated by the mass M_2 and a spring of stiffness K_2 . The surface can be replaced by a spring K_1 and an equivalent mass M_1 . The springs associated with the particle and the surface are to account for the compliance of the materials these are made up of.

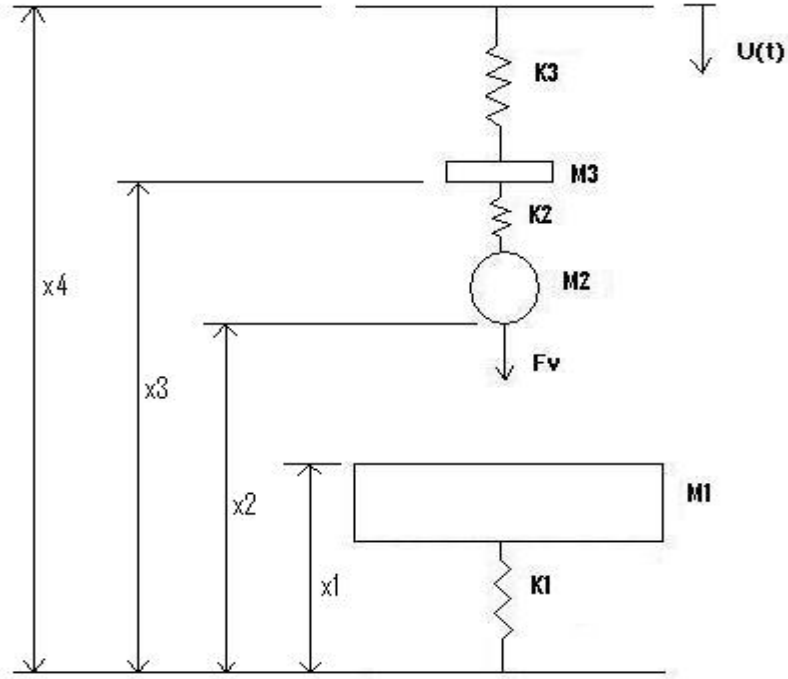


FIG. 16. Model for rigid particle.

The force between the particle and the surface (F_v) is approximated by Van der Waals adhesion forces, given by $F = \pi^2 C \rho^2 R / 6D^2$. These forces have been derived and explained in detail in section 4.4.

The end of the cantilever can be given any arbitrary motion $U(t)$. The equations of motion for the masses M_1 , M_2 and M_3 can be generated from basic kinematics. The explicit differential equations for the motion of the system are derived as explained below.

Considering the free body diagrams of the particle, the surface and the spring respectively, as shown in Fig. 17,

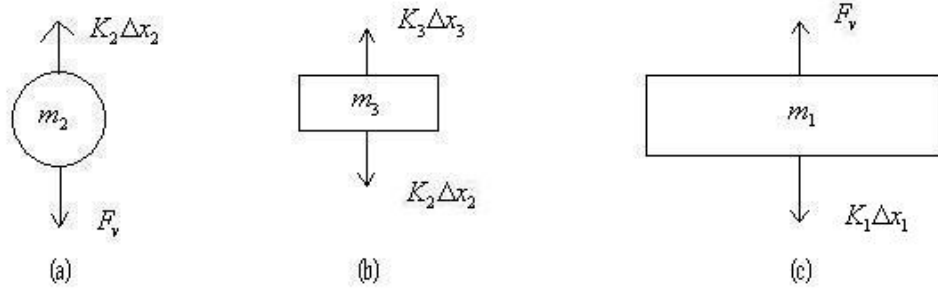


FIG. 17. Free body diagrams of (a) particle, (b) cantilever and (c) surface.

$$\begin{aligned}
 m_1 \ddot{x}_1 &= F_v - K_1(x_1 - L_1) \\
 m_2 \ddot{x}_2 &= -F_v + K_2\Delta x_2 = -F_v + K_2((x_3 - x_2) - L_2) \\
 m_3 \ddot{x}_3 &= K_3((x_4 - x_3) - L_3) - K_2((x_3 - x_2) - L_2)
 \end{aligned}$$

Where L_1 , L_2 and L_3 are the natural lengths of the three springs and rest of the parameters are as explained above.

For practical purposes, the stiffness of the surface can be neglected as it is assumed to be rigid in comparison to the particle. The stiffness and equivalent mass of both the cantilever and the particle need to be determined in order to be used in the model.

The stiffness of the cantilever is provided by the manufacturer. This value is taken as a standard. The equivalent mass of the cantilever can be found by finding its natural frequency. The natural frequency is found by using the ‘sweep’ command in tapping mode in AFM. The natural frequency of the cantilever is given

by $\omega_n = \sqrt{\frac{k}{m}}$ and thus mass is given by $m = \frac{K}{\omega_n^2}$.

The mass of the particle can be calculated by multiplying the density of the particle material with its volume. As the particle is a sphere, its volume is given by $V = \frac{4}{3}\pi R^3$ and thus the mass is $M = \frac{4}{3}\pi R^3 \rho$, where ρ is the density of the particle material. To find the equivalent stiffness of the particle, calculations are made for a sphere using Lagrangian approach for its strain energy. This derivation is shown in section 4.6.

4.6 Calculation of stiffness for spherical particle

To calculate the equivalent stiffness of the particle due to its compliance, we take the problem as follows. Let the un-deformed sphere have a radius 'R'. After deformation, we assume that the sphere becomes an ellipsoid with vertical dimension $R(1+a)$ and the horizontal dimension $R(1+b)$. This can be seen in Fig 18.

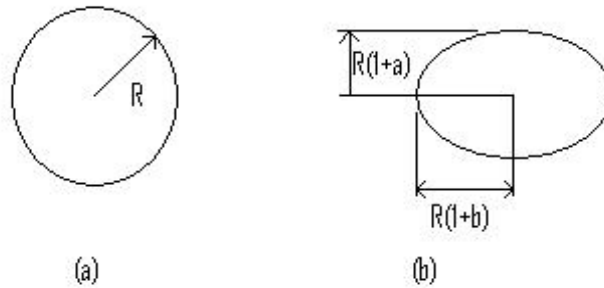


FIG. 18. Figure to show the (a) undeformed and (b) deformed particle.

The deformation gradient matrix for this configuration is given by:

$$F = \begin{pmatrix} a+1 & 0 & 0 \\ 0 & b+1 & 0 \\ 0 & 0 & b+1 \end{pmatrix}$$

And

$$\nabla u = F - I = \begin{pmatrix} a & 0 & 0 \\ 0 & b & 0 \\ 0 & 0 & b \end{pmatrix}$$

Where u is the displacement of a point in the body.

Infinitesimal strain (ε) is given by,

$$\varepsilon = \frac{1}{2}[\nabla u + \nabla u^T] = \begin{pmatrix} a & 0 & 0 \\ 0 & b & 0 \\ 0 & 0 & b \end{pmatrix}$$

For isotropic materials, the stress (σ) in the body for a given strain (ε) is given by the equation:

$$\sigma = 2\mu\varepsilon + \lambda \text{tr}(\varepsilon)I$$

Where μ and λ are Lamé's constants, given in terms of the Young's modulus (E) and Poisson's ratio (ν) as

$$\mu = \frac{E}{2(1+\nu)} \text{ And } \lambda = \frac{E\nu}{(1+\nu)(1-2\nu)}$$

So for this configuration, stress matrix is given by:

$$\sigma = \begin{pmatrix} 2\mu a + \lambda(a+2b) & 0 & 0 \\ 0 & 2\mu b + \lambda(a+2b) & 0 \\ 0 & 0 & 2\mu b + \lambda(a+2b) \end{pmatrix}$$

The strain energy of a body with stress σ and strain ε is given by:

$$U = \frac{1}{2} \int_V \sigma_{ij} \varepsilon_{ij} dV$$

Where V is the volume of the body.

Now for the given particle with given stress σ and strain ε ,

$$\begin{aligned} \sigma_{ij} \varepsilon_{ij} &= (2\mu a^2 + \lambda(a+2b)a) + (2\mu b^2 + \lambda(a+2b)b) + (2\mu b^2 + \lambda(a+2b)b) \\ &= 2\mu(a^2 + 2b^2) + \lambda(a+2b)^2 \end{aligned}$$

Therefore, taking the reference volume of the sphere as $V = \frac{4}{3}\pi R^3$, we get

$$U = \frac{2}{3}\pi(2\mu(a^2 + 2b^2) + \lambda(a+2b)^2)R^3$$

Now to get the stiffness, we use the Lagrangian approach.

Considering,

$$\frac{\partial U}{\partial b} = 0 \text{ and } \frac{\partial U}{\partial a} = PR, \text{ we can get the stiffness of the particle.}$$

$$\begin{aligned} \frac{\partial U}{\partial b} &= 0 \\ \Rightarrow 4\mu b + 2\lambda(a+2b) &= 0 \\ \Rightarrow b &= \frac{-a\lambda}{2(\mu + \lambda)} \end{aligned}$$

And

$$\begin{aligned}
\frac{\partial U}{\partial a} &= PR \\
\Rightarrow \frac{2}{3} \pi R^3 (4\mu a + 2\lambda(a + 2b)) &= PR \\
\Rightarrow \frac{4}{3} \pi R^3 \frac{\mu(2\mu + 3\lambda)}{(\lambda + \mu)} a &= PR \\
\frac{4}{3} \pi R \frac{\mu(2\mu + 3\lambda)}{(\lambda + \mu)} (aR) &= P
\end{aligned}$$

Solving for E from equations of λ and μ , we get

$$E = \frac{\mu(2\mu + 3\lambda)}{(\lambda + \mu)}$$

Therefore the equivalent stiffness of the spring is given by

$$K = \frac{4}{3} \pi R E$$

Where R is the radius of the un-deformed sphere and E is the Young's modulus of the sphere material.

4.7 Stiffness and mass for a given set of particle and cantilever

In this section, some equivalent stiffness and mass calculations are shown for a polystyrene particle of 20 micron diameter and a 100 micron wide cantilever.

Mass of particle (M):

$$V = \frac{4}{3} \pi R^3$$

$$M = \frac{4}{3} \pi R^3 \rho$$

The density of polystyrene is 1.04-1.07 g/cc. For our case we take it as 1.05 g/cc. Therefore for a 20 micron particle the mass is $M=4.395*10^{-12} \text{ Kg}$ or $.004395 \mu\text{g}$.

Equivalent stiffness of particle (K):

$$K = \frac{4}{3} \pi R E$$

The Young's modulus for Polystyrene is given as 3 GPa. Putting this in the stiffness for a 20 micron particle, we get $K= 1.251*10^5 \text{ N/m}$

Stiffness of cantilever (k):

This is given as a standard by the manufacturer. Here we take a 100 micron Wide cantilever, whose stiffness is given as $k=0.58 \text{ N/m}$

Equivalent mass of the cantilever(m):

As described in section 4.5, natural frequency of a 100 micron wide cantilever is found experimentally using the AFM. The natural frequency was found to be 1.39 KHz. Now the equivalent mass can be calculated using $m = \frac{K}{\omega_n^2}$ to be

$m=3.07*10^{-10} \text{ Kg}$ or $.307 \mu\text{g}$.

CHAPTER V

RESULTS AND DISCUSSION

5.1 Pull-off forces for particles of various sizes at a single frequency

There are two variables which affecting pull-off force that are studied in this work. These are particle size and frequency of pull-off. First we study the effect of particle size on the pull-off force. For this, the experiments were conducted at a constant frequency for many particles of different sizes. The force-displacement plots were obtained for each particle and from these plots, the pull-off force was calculated for each particle. These pull-off forces were plotted against particle size. This plot is seen in Fig. 19.

A line fitting the points on in the plot is drawn on the plot with Y intercept set as zero. The slope of this line is found to be 5.85 (nN/ μ m). Therefore the equation for pull-off force with particle size can be written as $F=5.85 \cdot R$, where F is pull-off force and R is the diameter of the particle.

There is one anomalous point in the 21 μ m range that has a very low pull-off force. On further verification it was found that the cantilever had got excess glue on the bottom. This cantilever can be seen in Fig. 20. This made the cantilever stiffer and thus the deflection of the tip was lower. This deflection when multiplied with the standard stiffness given by the manufacturer, gave a lower force.

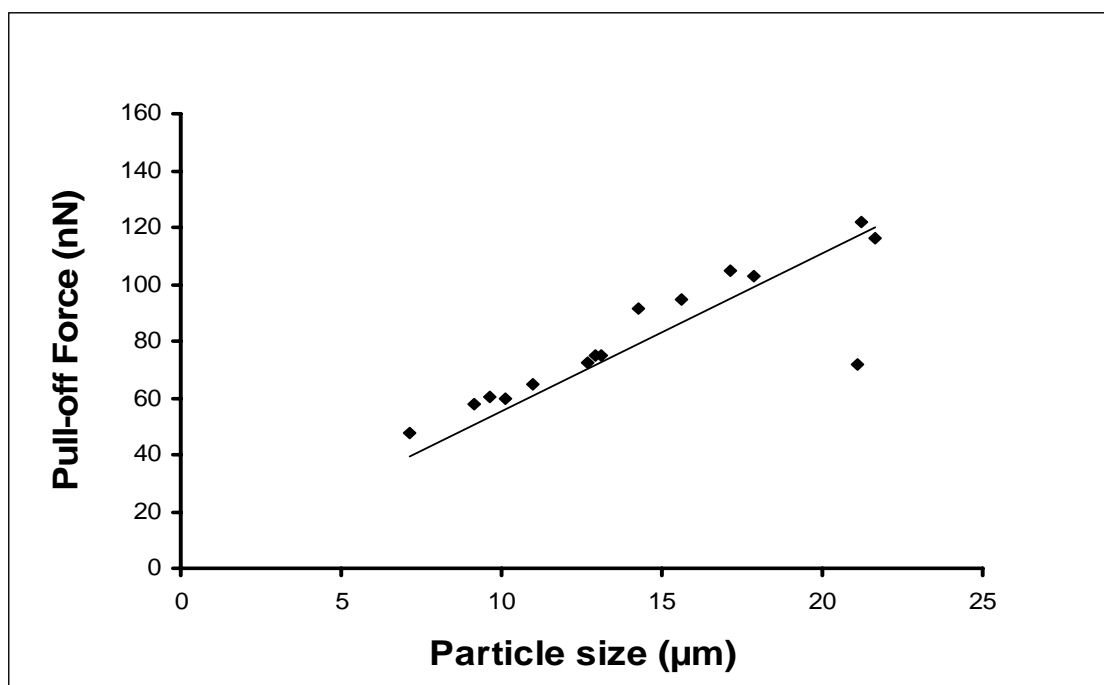


FIG. 19. Plot of pull-off force vs. particle size.

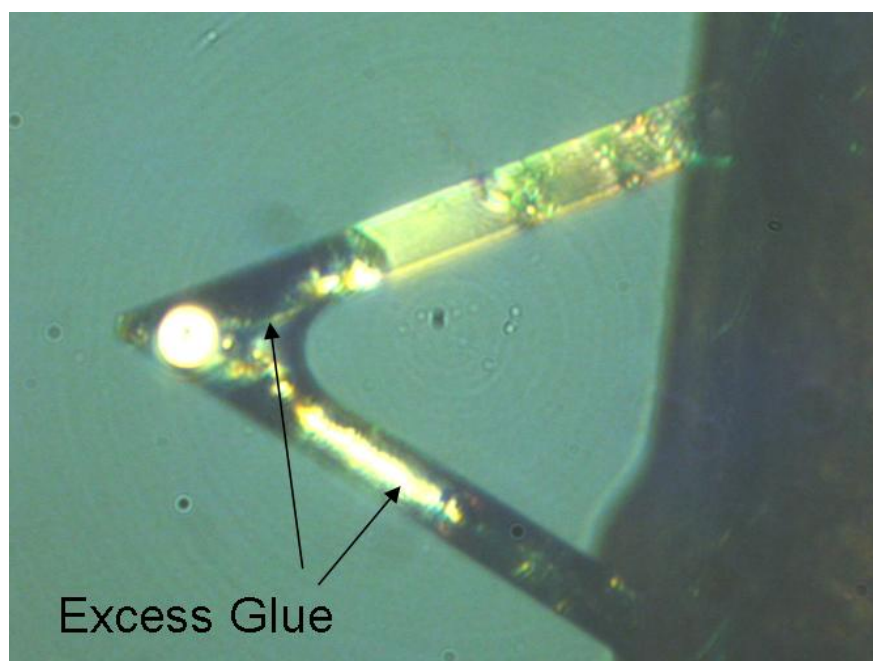


FIG. 20. Cantilever with particle. The cantilever had excess glue on the bottom face.

5.2 Pull-off force for varying frequency

Experiments were done with each particle for varying frequency. The force-displacement plots were obtained for each particle at each frequency. A frequency plot is shown in Fig. 21 for a particle of diameter $17.156\text{ }\mu\text{m}$.

Similar plots were obtained for each particle experimented on. These plots are combined in a single graph and are shown in Fig. 22.

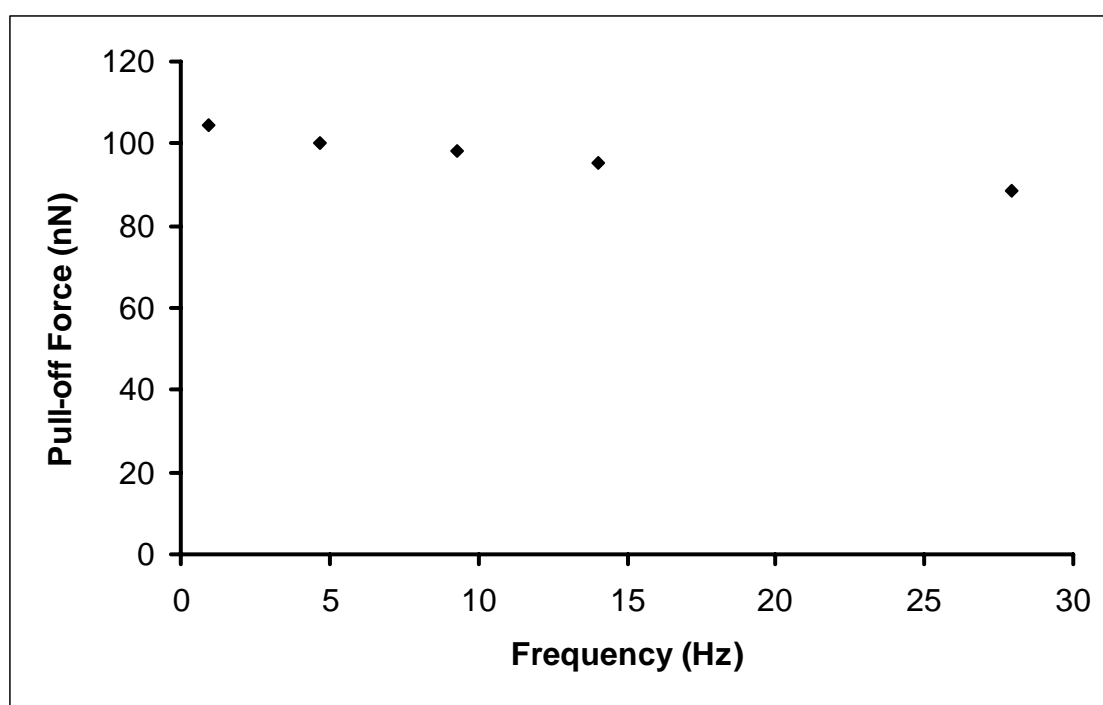


FIG. 21. Pull-off force vs. Frequency for a particle of diameter $17.156\text{ }\mu\text{m}$.

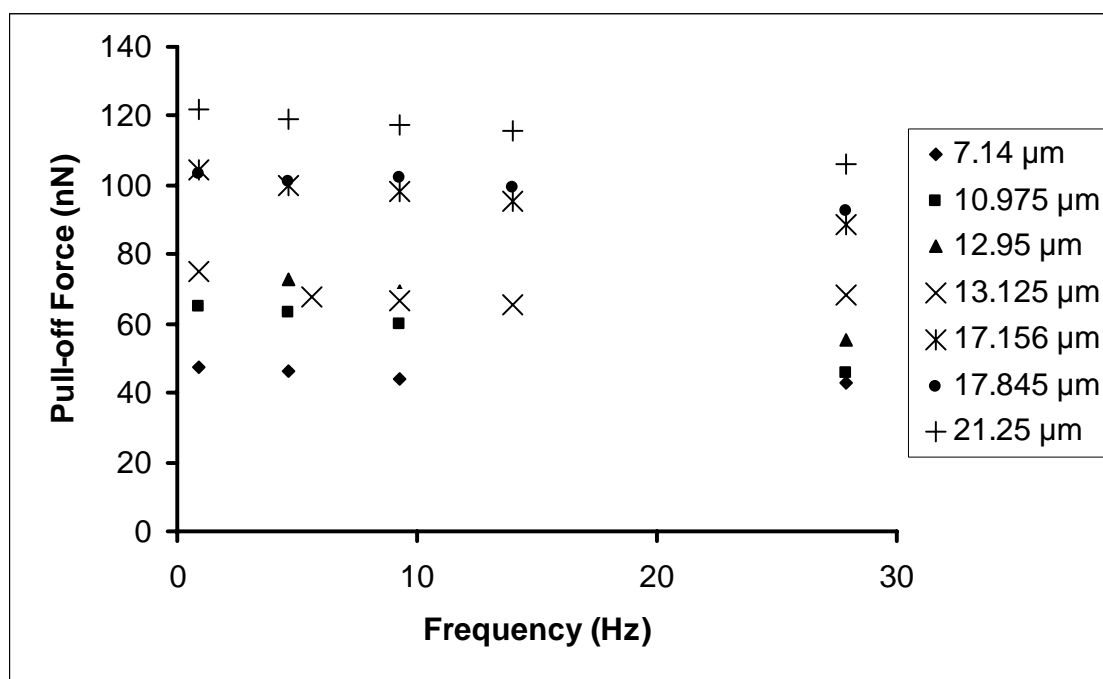


FIG. 22. Pull-off Force vs. Frequency for particles of varying sizes.

In the plot for Pull-off force vs. Particle size, it was found that the ratio of pull-off force with particle size would be almost a constant. This constant would be called 'R'. This constant can be found for all the single plots in the Fig. 22 above and the average value for each frequency is plotted against frequency. This plot is seen in Fig. 23.

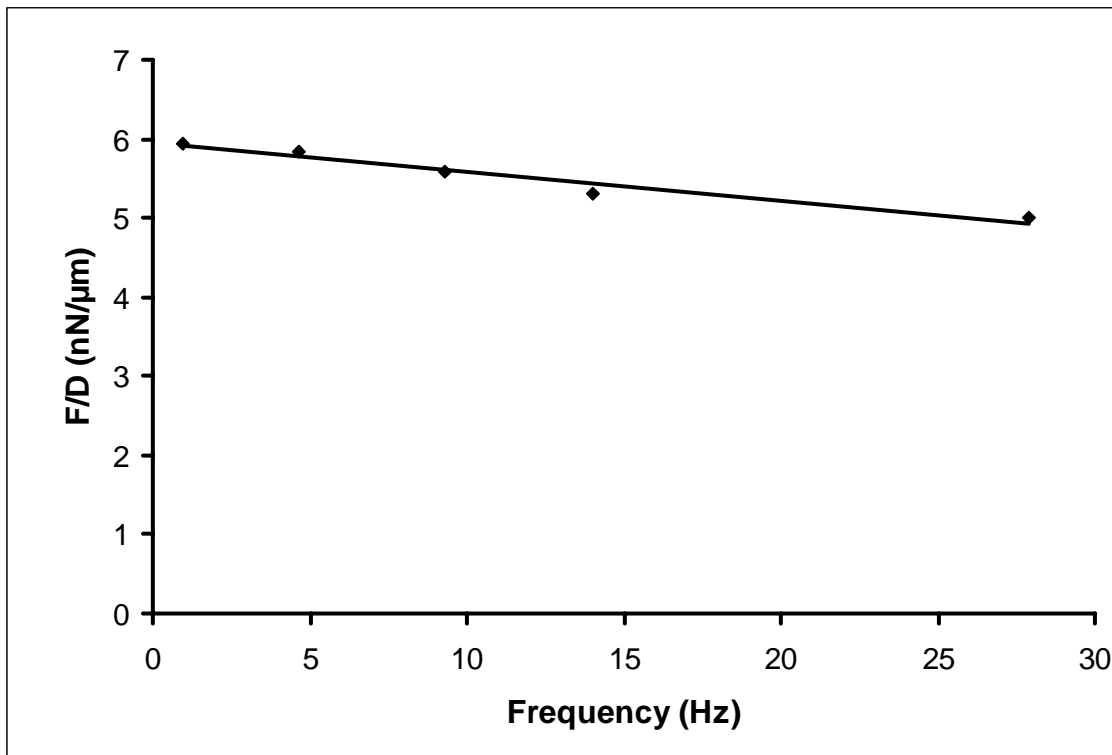


FIG. 23. Plot of the constant ‘Pull-off force/ Particle size’ vs. Frequency.

The slope of the line fitting the points in the plot shown in Fig. 23 above is $m = -0.0363$.

5.3 Discussion

The slope of the line that fits the pull-off force vs. particle diameter is found to be $5.85 \text{ (nN/}\mu\text{m)}$. This ratio i.e. pull-off force by particle diameter would be given by $3/4\gamma\pi$. The surface energy for polystyrene is approximately $.02\text{N/m}$ (37). Therefore the slope for JKR would be $47.12 \text{ nN/}\mu\text{m}$. The same value given by DMT

theory would be $\gamma\pi$. This value is 62.83 nN/ μm . The values obtained from the experiments do not match with the JKR and DMT theories.

The slope of the line from the frequency plot is -0.0363 (nN/ μm)/Hz. i.e. the value of the ratio R (which is equal to pull-off force by particle diameter) reduces by -0.0363 nN/ μm for an increase of frequency by 1 Hz. In the experiments the velocity profile of the tip displacement is a saw-tooth profile with amplitude 5 μm . This corresponds to an equation for velocity given by $V=10 \cdot F \mu\text{m/s}$, where F is the frequency.

Therefore the equation for ratio 'R' with pull-off velocity 'V' is given by $R=5.9443 - 0.0036V$. Using this equation, the ratio 'R' can be determined for velocities higher than those which can be measured by the AFM.

REFERENCES

1. Das, S. K. and Sharma, M. M., in “Particles on Surfaces 5 & 6: Detection, Adhesion and Removal” (K. L. Mittal, Ed.), pp. 149-186. VSP, Utrecht, Netherlands, 1999.
2. Paiva, A., Sheller, N., Foster, M. D., Crosby, A. J., and Shull, K. R., *Macromolecules* **33**, 1878 (2000).
3. Lam, K. L., and Newton, J. M., *Powder Technol.* **73**, 267 (1992).
4. Frank, B. P., and Belfort, G., *Langmuir* **17**, 1905 (2001).
5. Bowen, W. R, and Doneva, T. A., *J. Colloid Interface Sci.* **229**, 544 (2000).
6. Sengeren, L. J. G. H., Karssenberg, F. G., Pickering, J. P., Van Den Berg, J. W. A., and Vancso, G. J., in “Particles on Surfaces 7: Detection, Adhesion and Removal” pp. 197-217. VSP, Utrecht, Netherlands, 2002.
7. Bleach, E., Drelich, J., and Han, R., in “Particles on Surfaces 7: Detection, Adhesion and Removal” pp. 219-234. VSP, Utrecht, Netherlands, 2002.
8. Segeren, L. J. G. H., Seibum, B., Karssenberg, F. G., Van Den Berg, J. W. A., and Vancso, G. J., *J. Adhesion Sci. Technol.* **16**, 793 (2002).
9. Rabinovich, Y. I., Adler, J. J., Ata, A., Singh, R. K., and Moudgil, B. M., *J. Colloid Interface Sci.* **232**, 17 (2000).
10. Cooper, K., Gupta, A., and Beaudoin, S., *J. Colloid Interface Sci.* **228**, 213 (2000).

11. Sirghi, L., Nakagiri, N., Sugisaki, K., Sugimura, H., and Takai, O., *Langmuir* **16**, 7796 (2000).
12. Mizes, H. A., Loh, K. G., Miller, R. J. D., Ahuja, S. K., and Grabowski, E. F., *Appl. Phys. Lett.* **59**, 2901 (1991).
13. Israelachvili, J., “Intermolecular and surface forces, 2nd edition,” Academic Press, London, 1991.
14. Johnson, K. L., and Greenwood, J. A., *J. Colloid Interface Sci.* **192**, 326 (1997).
15. Quon, R. A., Ulman, A., and Vanderlick, T. K., *Langmuir* **16**, 8912 (2000).
16. Attard, P., *Langmuir* **17**, 4322 (2001).
17. Johnson, K. L., Kendall, K., and Roberts, A. D., *Proc. R. Soc. London, A: Math. Phys. Sci.* **324**, 301 (1971).
18. Derjaguin, B. V., Muller, and V. M., Toporov, Y. P., *J. Colloid Interface Sci.* **53**, 314 (1975).
19. Duijvenbode, R. C. v., and Koper, G. J. M., *J. Colloid Interface Sci.* **239**, 581 (2001).
20. Falsafi, A., Tirrell, M., and Pocius, A. V., *Langmuir* **16**, 1816 (2000).
21. Binnig, G., Quate, C. F., and Gerber, Ch., *Phys. Rev. Lett.* **56**, 930 (1986).
22. “Nanoscope Command Reference Manual”, Veeco Metrology Group Inc., Chadds Ford, Pennsylvania, 1999.
23. Ducker, W. A., Senden, T. J., and Pashley, R. M., *Nature* **353**, 239 (1991).

24. Schönherr, H., Beulen, M. W. J., Bügler, J., Huskens, J., van Veggel, F. C. J. M., Reinhoudt, D. N., and Vansco, G. J., *J. Am. Chem. Soc.* **122**, 4963 (2000).
25. Portigliatti, M., Koutsos, V., Hervet, H., and Léger, L., *Langmuir* **16**, 6374 (2000).
26. Gady, B., Schleef, D., Reifenberger, R., Ramai, D., and DeMejo, L. P., *Phys. Rev. B* **53**, 8065 (1996).
27. Willing, G. A., Ibrahim, T. H., Etzler, F. M., and Neuman, R. D., *J. Colloid Interface Sci.* **226**, 185 (2000).
28. Chan, D. Y. C., Dagastine, R. R., and White, L. R., *J. Colloid Interface Sci.* **236**, 141 (2001).
29. Gotzinger, M., and Peukert, W., *Powder Technology* **130**, 102 (2003).
30. Schönherr, H., Hruska, Z., and Vansco, G. J., *Macromolecules* **31**, 3679 (1998).
31. Cooper, K., Gupta, A., and Beaudoin, S., *J. Colloid Interface Sci.* **234**, 284 (2001).
32. Cleasson, P. M., Ederth, T., Bergeron, V., and Rutland, M. W., *Adv. Colloid Interface Sci.* **67**, 119 (1996).
33. Hertz, H., "Miscellaneous Papers", pp. 146. Macmillan, London, 1896.
34. Maugis, D., *J. Colloid Interface Sci.* **150**, 243 (1992).
35. Ramai, D. S., DeMejo, L. P., and Bowen, R. C., *J. Appl. Phys.* **66**, 3574 (1989).

36. Feng, J. Q., *J. Colloid Interface Sci.* **238**, 318 (2001).
37. Kwok, D. Y., and Neumann, W. A., in “Contact Angle, Wettability and Adhesion”, (K. L. Mittal, Ed.), pp. 117-159. VSP, Utrecht, Netherlands, 2003.

VITA

Name: Anshul Kaushik

Address: 4303 Boyett St., Apt 'B'
Bryan,
Texas – 77801, USA.

Date of birth: Aug. 28, 1980.

Education:

2002-2004	Texas A&M University Master of Science Mechanical Engineering, 2004.
1998-2002	M.V.S.R Engineering College Osmania University Hyderabad, India. Bachelor of Engineering, Mechanical Engineering, 2002.